White Rose Research Online

eprints@whiterose.ac.uk
https://eprints.whiterose.ac.uk
Universities of Leeds, Sheffield and York

Deposited via The University of Sheffield.

White Rose Research Online URL for this paper:
https://eprints.whiterose.ac.uk/id/eprint/196800/

Version: Accepted Version

Article:
Yang, Z., Shen, Q., Liu, W. et al. (2023) High-order cumulants based sparse array design via fractal geometries—part I: structures and DOFs. IEEE Transactions on Signal Processing, 71 (2023). pp. 327-342. ISSN: 1053-587X

https://doi.org/10.1109/tsp.2023.3244672

© 2023 IEEE. Personal use of this material is permitted. Permission from IEEE must be obtained for all other users, including reprinting/ republishing this material for advertising or promotional purposes, creating new collective works for resale or redistribution to servers or lists, or reuse of any copyrighted components of this work in other works. Reproduced in accordance with the publisher's self-archiving policy.

Reuse
Items deposited in White Rose Research Online are protected by copyright, with all rights reserved unless indicated otherwise. They may be downloaded and/or printed for private study, or other acts as permitted by national copyright laws. The publisher or other rights holders may allow further reproduction and re-use of the full text version. This is indicated by the licence information on the White Rose Research Online record for the item.

Takedown
If you consider content in White Rose Research Online to be in breach of UK law, please notify us by emailing eprints@whiterose.ac.uk including the URL of the record and the reason for the withdrawal request.

UNIVERSITY OF LEEDS
University of Sheffield
UNIVERSITY of York

High-Order Cumulants Based Sparse Array Design via Fractal Geometries—Part I: Structures and DOFs

Zixiang Yang, Qing Shen, Wei Liu, *Senior Member, IEEE,* Yonina C. Eldar, *Fellow, IEEE,* Wei Cui

***Abstract*—Array structures based on the high-order difference co-array concept provide a large number of degrees of freedom, but are typically difficult to design under multiple optimality criteria. In this paper, we present a joint across-order (across different cumulant order q) and inner-order (within the same cumulant order q) fractal framework to form a fractal array based on the $2q$th-order difference co-array ($2q$th-O-Fractal) by recursively using a simple generator. We show that multiple properties of interest, including large consecutive difference co-array, closed-form sensor positions, hole-free difference co-array, robustness to sensor failures, and resilience to mutual coupling, are inherited from the generator under appropriate conditions. Part I of the work focuses on array structures with a large uniform or hole-free (higher-order) difference co-array. First, we show that for an array of size N, $\mathcal{O}(N^{2q})$ consecutive co-array lags can be provided by optimizing the generator. In addition, the generated structure outperforms existing structures in terms of the number of consecutive lags offered. Then, proof is provided that under given requirements on the generator, the hole-free property is inherited for $q = 2$, and $\mathcal{O}(N^4)$ hole-free fourth-order difference co-array lags can be achieved by the proposed framework, which is larger than those of existing structures. Simulation results verify the superiority of the proposed framework in terms of estimation accuracy and resolution capability. Part II of this work focuses on the properties of array robustness and mutual coupling.**

***Index Terms*—Sparse array design, difference co-array, high-order cumulants, fractal geometry, direction of arrival estimation.**

I. Introduction

Array signal processing plays an important role in the fields of radar, sonar, communications and radio astronomy [1]–[4], where array geometry design is one of the core issues. Sparse linear arrays with non-uniform inter-element spacings have the ability to resolve more uncorrelated sources than the number of physical sensors in direction of arrival (DOA) estimation [2], [5], [6]. The virtual array constructed by using the second-order [2], [7], or high-order statistics [8], [9], of the received signals contributes to this capability. Due to this advantage, a series of array structure design criteria and methods have been proposed over the past decade.

For second-order statistics based DOA estimation, the number of degrees of freedom (DOFs) is closely related to the second-order difference co-array of the physical array. Minimum redundancy array (MRA) [10] is a well-known early structure, which pursues a large number of DOFs by minimizing the number of redundant sensor positions. The non-closed form expressions of sensor positions limit the scalability of MRA, increasing the difficulty in large-scale array design. Subsequently, nested array (NA) [2] and coprime array (CPA) [5] structures were studied extensively due to their large difference co-arrays and closed-form expressions of sensor positions. NA and CPA have triggered an upsurge of follow-up works, which focus on further improving the number of DOFs, such as augmented coprime array (ACA) [11], improved nested array (INA) [12], enhanced nested array (ENA) [13], and array based on the maximum element spacing criterion (MISC) [14], [15]. In traditional subspace-based methods [16], only information from the continuous segment of the difference co-array is utilized, so that a hole-free difference co-array is beneficial. Hole-filling strategies were suggested to form new CPA-like array structures with a hole-free difference co-array [17]–[20].

Due to the dense first-level subarray in NA [21], the estimation performance of NA deteriorates sharply in the presence of mutual coupling [22]. In order to reduce mutual coupling, a series of improved structures have been proposed [21], [23]–[26]. Most of these techniques keep the number of DOFs provided unchanged or even improved [23], [24], [26]. On the other hand, considering the possibility of physical sensor damage, the robustness of sparse arrays and stability of co-arrays have been discussed recently [27]–[29], while structures with improved robustness are presented in [30]–[32].

Evidently, sparse array design has to address multiple constraints rather than a single criterion for achieving a large consecutive difference co-array, and appropriate balance among various criteria is often needed. One solution is sparse array design via fractal geometry [33] with inherent self-similarity [34]–[36]. In [3], [37], the proposed fractal array inherits a variety of properties from its simple generator, including properties of large consecutive difference co-array, hole-free difference co-array, robustness, and low coupling leakage, leading to high flexibility in multi-criterion joint design.

The aforementioned works are all based on second-order statistics leading to difference co-arrays. High-order cumulant-

This work was supported in part by the National Natural Science Foundation of China under Grant 62271052. (Corresponding author: Qing Shen.)

Z. Yang, Q. Shen and W. Cui are with the School of Information and Electronics, Beijing Institute of Technology, Beijing, 100081, China (e-mail: zixiangyang@foxmail.com, qing-shen@outlook.com, cuiwei@bit.edu.cn)

W. Liu is with the Department of Electronic and Electrical Engineering, University of Sheffield, Sheffield, S1 3JD, UK (e-mail: w.liu@sheffield.ac.uk).

Y. C. Eldar is with the Faculty of Mathematics and Computer Science, Weizmann Institute of Science, Rehovot, Israel (e-mail: yonina.eldar@weizmann.ac.il).

based methods have been extensively studied within the field of DOA estimation [8], [38]–[45], offering increased virtual array aperture, improved resolution capability, estimation accuracy, and robustness against Gaussian noise [8], [40], [44], compared with methods based on second-order statistics. Although these techniques are not applicable to Gaussian sources and have higher computational complexity, many real-world signals are non-Gaussian [39]. Thus, methods based on high-order cumulants have been employed in many applications due to their advantages mentioned above. For example, these methods are typical solutions to direction finding problems in wireless communication systems [38], [44] and acoustic systems [45], [46]. By vectorizing an arbitrary even order ($2q$) cumulant matrix of the received data, a virtual array model is obtained with its virtual sensor set defined as the $2q$th-order difference co-array [8]. For an N-sensor array, there are N^{2q} virtual elements (including redundant ones) in its $2q$th-order difference co-array. However, the unique co-array elements related to the DOFs rely on the physical array geometry, raising the array design problem incorporating different properties. A well-designed geometry should offer $\mathcal{O}(N^{2q})$ DOFs that can be exploited by high-order cumulant-based methods, which is far more than $\mathcal{O}(N^2)$ when second-order statistics based techniques are considered.

In [8], a $2q$-level nested array ($2q$L-NA) providing $\mathcal{O}(N^{2q})$ DOFs with N physical sensors is proposed, which is the first structure designed based on the $2q$th-order difference co-array. By optimizing the redundant co-array lags in $2q$L-NA, a simplified and enhanced $2q$-level nested array (SE-$2q$L-NA) with increased DOFs was derived [9]. Only the criterion of achieving large consecutive $2q$th-order difference co-array with closed-form expressions of sensor positions is adopted in designing $2q$L-NA and SE-$2q$L-NA. However, the mutual coupling is relatively high due to the NA-like structure. A number of sparse structures have been proposed specifically for fourth-order ($q = 2$), including the expanding and shift (EAS) array structure [47], sparse array with fourth-order difference co-array enhancement based on a nested array (SAFO-NA) [48], two level nested sparse array (2L-FO-NA) [49], compressed nested array (CNA) [50], and generalized CNA (GCNA) [51], where 2L-FO-NA, CNA, and GCNA offer hole-free fourth-order difference co-arrays with $\mathcal{O}(N^2)$ DOFs. For E-FO-Cantor [52], the number of DOFs is increased to $\mathcal{O}(N^{3.17})$ under the premise of satisfying the hole-free property, shortening the gap toward $\mathcal{O}(N^4)$ provided by $2q$L-NA ($q = 2$) and SE-$2q$L-NA ($q = 2$) without hole-free co-arrays.

Compared with array structures exploiting the second-order difference co-array, flexible sparse array design in the higher-order case is much less investigated. Most existing works only focus on the property of large DOFs. Sparse array design incorporating multiple criteria based on the $2q$th-order difference co-array is difficult due to the extremely large number of co-array lags (N^{2q} including redundancies) involved in the optimization.

Inspired by the flexible fractal framework proposed in [3], [37], we introduce commonly adopted criteria to sparse array design based on the $2q$th-order difference co-array, and present a joint across-order (across different cumulant order q) and inner-order (within the same cumulant order q, referred to as fractal order r) fractal framework to form a fractal array exploiting the $2q$th-order difference co-array ($2q$th-O-Fractal). Different from existing structures where only fractal factor r for $q = 1$ (inner-order) is considered, both fractal factors q and r are related to the designed array configurations via fractal geometries, and are considered in the analysis. In this proposed simple systematic framework, any sparse linear structure can be treated as a generator, recursively expanded to generate a large array for the $2q$th-order difference co-array exploitation with multiple properties inherited from the generator. Therefore, by optimizing the generator array according to given criteria, the associated $2q$th-O-Fractal can be easily obtained incorporating multiple properties of interest, leading to a flexible framework for joint multi-criterion design.

Part I of this work is focused on the following contributions:

1) A joint across-order and inner-order fractal framework is proposed to generate a fractal array based on the $2q$th-order difference co-array, leading to $2q$th-O-Fractal whose properties are inherited from its optimized generator. The properties of interest include large consecutive difference co-array, closed-form expression, hole-free difference co-array, robustness and economy, and low mutual coupling.

2) The large consecutive difference co-array criterion is considered, which was the main metric for array construction based on the $2q$th-order difference co-array in the past. In contrast to existing structures exploiting the nested idea to design higher level uniform linear subarrays with different spacings [8], [9], the proposed $2q$th-O-Fractal is sparser with reduced redundancies and flexible configurations. By inheriting the property of a large consecutive difference co-array from its generator, we prove that $2q$th-O-Fractal is capable of providing uniform DOFs of $\mathcal{O}_c(C_F N^{2q})$ with a larger coefficient C_F compared with existing structures, and improved performance in terms of resolution capability and estimation accuracy can be achieved. Here $\mathcal{O}_c(C_F N^{2q})$ means $C_F N^{2q}$ is asymptotically achieved when N tends to infinity. It is also proved that for a large sensor number N, the ratio of the number of uniform DOFs provided by $2q$th-O-Fractal to that provided by existing structures increases exponentially with order q.

3) For $q = 2$, the requirement for the generator is given to ensure the inheritance of hole-free property, leading to 4th-O-Fractal with $\mathcal{O}(N^4)$ DOFs provided by hole-free fourth-order difference co-array, which is larger than that of existing structures ($\mathcal{O}(N^2)$ by 2L-FO-NA, CNA, and GCNA, and $\mathcal{O}(N^{3.17})$ by E-FO-Cantor). A series of structures are then given by choosing various types of generator arrays which are proved to satisfy the mentioned requirement.

This paper is organized as follows. Section II provides basics about sparse array design, including signal model, high-order difference co-array, and design criteria. The proposed fractal array based on the $2q$th-order difference co-array is detailed in Section III, and the conditions of achieving large consecutive difference co-array and hole-free property are analyzed in Section IV. Comparisons and simulation results are given in Section V, while conclusions are drawn in Section

VI.

II. Preliminaries of Sparse Array Design

A. Signal Model

Consider K narrowband far-field sources impinging on a linear array, and assumed to be non-Gaussian and independent of each other. The set of K incident angles is represented by $\boldsymbol{\theta} = \{\theta_1, \theta_2, \cdots, \theta_K\}$. The sensor position set of an arbitrary linear array with N physical sensors is

$$\mathbb{A} = \big\{p_n \cdot d \mid n \in [1, N]\big\}, \tag{1}$$

where $p_n d$ denotes the position of the n-th sensor, and d is the unit spacing which is omitted hereafter for simplification.

The received signals from N sensors are stacked to form an $N \times 1$ signal vector $\mathbf{x}[i]$. The array output model in discrete version is expressed as

$$\mathbf{x}[i] = \mathbf{A}(\boldsymbol{\theta})\mathbf{s}[i] + \mathbf{n}[i], \tag{2}$$

where the steering matrix $\mathbf{A}(\boldsymbol{\theta})$ is composed of K column vectors whose k-th column vector $\mathbf{a}(\theta_k)$ is the steering vector of the k-th source

$$\mathbf{a}(\theta_k) = \Big[e^{-j\frac{2\pi p_1 d \sin\theta_k}{\lambda}}, \cdots, e^{-j\frac{2\pi p_N d \sin\theta_k}{\lambda}}\Big]^T. \tag{3}$$

The signal vector $\mathbf{s}[i] = \big[s_1[i], s_2[i], \ldots, s_K[i]\big]^T$ with $\{\cdot\}^T$ being the transpose operator contains all source signals, and $\mathbf{n}[i]$ represents Gaussian white noise.

B. The $2q$th-Order Cumulant and Virtual Array

For a given structure, DOA estimation methods based on the $2q$th-order cumulants possess better identifiability than second-order statistics based methods [8], [43], [44]. A larger difference virtual array can be generated by vectorizing the cumulant matrix [8].

The $2q$th-order circular cumulants of the signal vector $\mathbf{x}[i]$ can be arranged in an $N^q \times N^q$ cumulant matrix with orientation u $\big(u \in [0, q-1]\big)$, i.e. [9], [53],

$$\mathbf{C}_{2q,\mathbf{x}}(u) = \sum\nolimits_{k=1}^{K} c_{2q,s_k} \Big[\mathbf{a}(\theta_k)^{\otimes u} \otimes \mathbf{a}(\theta_k)^{*\otimes(q-u)}\Big] \times \Big[\mathbf{a}(\theta_k)^{\otimes u} \otimes \mathbf{a}(\theta_k)^{*\otimes(q-u)}\Big]^H + \sigma_{\bar{n}}^2 \mathbf{I}_{N^q} \cdot \delta(q-1). \tag{4}$$

Here, $\otimes$, $\{\cdot\}^*$, $\{\cdot\}^H$, $\sigma_{\bar{n}}^2$, $\mathbf{I}_{N^q}$, and $\delta(\cdot)$ denote the Kronecker product, conjugate operator, conjugate transpose operator, noise power, the $N^q \times N^q$ identity matrix, and the Kronecker delta function, respectively. The $2q$th-order circular auto-cumulant of the k-th source signal $s_k[i]$ is given as

$$c_{2q,s_k} = \mathrm{Cum}\big\{\underbrace{s_k[i], \ldots, s_k[i]}_{q \text{ times}}, \overbrace{s_k^*[i], \ldots, s_k^*[i]}^{q \text{ times}}\big\}, \tag{5}$$

where $\mathrm{Cum}\{\cdot\}$ represents the cumulant operator, and the $N^u \times 1$ vector $\mathbf{a}(\theta_k)^{\otimes u}$ is defined as

$$\mathbf{a}(\theta_k)^{\otimes u} \triangleq \mathbf{a}(\theta_k) \otimes \mathbf{a}(\theta_k) \otimes \ldots \otimes \mathbf{a}(\theta_k), \tag{6}$$

with the Kronecker product $\otimes$ utilized $u-1$ times.

Vectorizing the cumulant matrix $\mathbf{C}_{2q,\mathbf{x}}(u)$ yields [8], [9]

$$\mathbf{z} = \mathrm{vec}\{\mathbf{C}_{2q,\mathbf{x}}(u)\} = \mathbf{V}(\boldsymbol{\theta})\mathbf{p} + \sigma_{\bar{n}}^2 \bar{\mathbf{i}}_{N^q} \cdot \delta(q-1). \tag{7}$$

In (7), a virtual array is generated by matrix vectorization, where $\mathbf{p} = [c_{2q,s_1}, c_{2q,s_2}, \cdots, c_{2q,s_K}]$ is the equivalent signal vector holding the $2q$th-order auto-cumulants of K sources, the column vector $\bar{\mathbf{i}}_{N^q} = \mathrm{vec}\{\mathbf{I}_{N^q}\}$, and

$$\mathbf{V}(\boldsymbol{\theta}) = \big[\mathbf{v}(\theta_1), \mathbf{v}(\theta_2), \cdots, \mathbf{v}(\theta_K)\big] \tag{8}$$

is the equivalent steering matrix with

$$\mathbf{v}(\theta_k) = \Big[\mathbf{a}(\theta_k)^{\otimes u} \otimes \mathbf{a}(\theta_k)^{*\otimes(q-u)}\Big]^* \otimes \Big[\mathbf{a}(\theta_k)^{\otimes u} \otimes \mathbf{a}(\theta_k)^{*\otimes(q-u)}\Big]. \tag{9}$$

The array output model in (7) is a general single-snapshot array model. The equivalent steering matrix $\mathbf{V}(\boldsymbol{\theta})$ is the virtual array manifold composed of virtual sensors located in the set of the $2q$th-order difference co-array, which is defined below. As proved in [8], $\mathbf{V}(\boldsymbol{\theta})$ is independent of the orientation u. Existing spatial-smoothing MUSIC (SS-MUSIC) as well as CS-based methods can be applied to this single-snapshot array model in (7) directly for DOA estimation [8], [9].

Definition 1: The $2q$th-order difference co-array [8], [9] for a linear array $\mathbb{A}$ is defined as

$$\mathbb{D}_{2q} = \Big\{\sum\nolimits_{k=1}^{q} \mu_k - \sum\nolimits_{l=q+1}^{2q} \mu_l \mid \mu_k,\ \mu_l \in \mathbb{A}\Big\}. \tag{10}$$

For an N-sensor physical array, the number of difference co-array lags in $\mathbb{D}_{2q}$ is N^{2q} including redundancies, implying that N^{2q} is an upper bound on the cardinality of $\mathbb{D}_{2q}$. No array can have more than $\mathcal{O}(N^{2q})$ elements in its $2q$th-order difference co-array. It has been shown in [8], [9] that $\mathcal{O}(N^{2q})$ co-array elements can be achieved for a specifically designed sparse array, which is larger than $\mathcal{O}(N^2)$ provided by the set of the second-order difference co-array ($q = 1$).

C. Criteria for Sparse Array Design

The number of DOFs of a linear array $\mathbb{A}$ exploiting the $2q$th-order difference co-array is the cardinality of $\mathbb{D}_{2q}$, i.e., $|\mathbb{D}_{2q}|$ [8], [9]. Let $\mathbb{U}_{2q}$ denote the central ULA segment of $\mathbb{D}_{2q}$. The cardinality of $\mathbb{U}_{2q}$ ($|\mathbb{U}_{2q}|$) is referred to as the number of uniform DOFs (uDOFs) [23].

Definition 2: The central ULA segment [3], [27] of the $2q$th-order difference co-array is the longest completely contiguous ULA symmetric about 0 in $\mathbb{D}_{2q}$, that is,

$$\mathbb{U}_{2q} \triangleq \arg \max_{\mathbb{U}_{l(2q)} \subseteq \mathbb{D}_{2q}} |\mathbb{U}_{l(2q)}|,$$
$$\mathbb{U}_{l(2q)} \triangleq \{-l, \cdots, -1, 0, 1, \cdots, l\}, \tag{11}$$

where l is a non-negative integer.

In the commonly used subspace-based methods such as SS-MUSIC [2], [8], [16], only the central ULA segment of the difference co-array can be utilized [8]. Therefore, the number of uDOFs generally has a great impact on the estimation performance [8], [23], and it is usually adopted as a metric for quantitative evaluation, comparison, and optimal design [9], [21], [54]. Therefore, we introduce the criterion of forming a

large consecutive difference co-array with high uDOFs in the sparse array design.

Criterion 1 (Large consecutive difference co-array): The number of uDOFs provided by the sparse array exploiting the $2q$th-order difference co-array should be $\mathcal{O}(N^{2q})$, where N is the number of physical sensors [2], [8], [9].

For the representation of the array structure, we prefer it to be in closed form.

Criterion 2 (Closed-form sensor positions): A closed-form expression of sensor positions is preferred for scalability considerations [3], [37].

The hole-free property is also desired in sparse array design. The co-array of a sparse array that satisfies the hole-free property is a virtual ULA. Next, the definition of the hole-free $2q$th-order difference co-array and the corresponding design criterion are provided.

Definition 3: The $2q$th-order difference co-array is defined to be hole-free if $\mathbb{D}_{2q} = \mathbb{U}_{2q}$ [3], [27].

Criterion 3 (Hole-free difference co-array): The cardinality of the central ULA segment reflects the number of sources resolved by the subspace-based DOA methods such as SS-MUSIC [3]. A sparse array having a hole-free difference co-array is preferred, since all information from its difference co-array can be utilized directly by subspace-based DOA methods which are easy to implement, and thus CS-based algorithms [21], [55]–[57] or co-array interpolation based techniques [58], [59] with increased overall complexity can be avoided [3], [7], [52].

In recent studies, considerations based on practical applications have received more attention. Typically, the mutual coupling effect [21]–[23] and the influence of element loss [27], [28] are analyzed in DOA estimation. These practical factors prompt us to consider *Criterion 4 (Robustness and economy)* and *Criterion 5 (Low mutual coupling)*, which will be introduced, discussed, and analyzed in the companion Part II [60].

In array design based on second-order statistics, a balance is achieved among multiple criteria. For example, super nested array (SNA) [23], [24] is designed according to *Criteria 1-3* and *Criterion 5*; robust MRA (RMRA) [30] is designed according to *Criteria 1*, *3*, and *4*; Cantor array [7] is designed according to *Criteria 2*, *3*, and *4*. The recently proposed fractal array inherits multiple properties from its simple generator array, and thus it is a generalized flexible array construction scheme via multi-criterion joint design [3].

In the design of sparse arrays exploiting $2q$th-order difference co-arrays, only one or two criteria have been considered in the literature. Two representative structures, i.e., $2q$L-NA [8] and SE-$2q$L-NA [9], are designed based on *Criteria 1* and *2*. In the special case of $q = 2$, several array configurations including 2L-FO-NA [49], CNA [50], and GCNA [51] are designed based on *Criteria 2* and *3*. Optimizing the sparse array configuration with closed-form sensor positions and a large hole-free difference co-array (*Criteria 1-3*) is a difficult problem. The E-FO-Cantor [52] offers $\mathcal{O}(N^{3.17})$ hole-free fourth-order difference co-array lags, which narrowing the gap toward $\mathcal{O}(N^4)$ claimed in *Criterion 1* compared with existing structures satisfying *Criteria 2* and *3*.

In the following, the fractal idea for sparse array design is introduced based on higher-order statistics, and the popular properties of the proposed structure (including the number of uDOFs, potential hole-free difference co-array, robustness, and mutual coupling effect) are analyzed, showing property inheritance with the generator array and flexibility in joint multi-criterion design. The new structure and discussions on the number of uDOFs and hole-free property are presented in this part, while the companion Part II focuses on the analysis of array robustness and the mutual coupling effect [60].

III. Fractal Arrays Based on the $2q$th-Order Difference Co-Array

A. Fractal Array Based on the Difference Co-Array

Fractal arrays based on the difference co-array (also known as the second-order difference co-array) with a generator array $\mathbb{G}$, referred to as SO-Fractal, are constructed as [3], [37]

$$\begin{aligned} \mathbb{F}_0 &\triangleq \{0\}, \\ \mathbb{F}_{r+1} &\triangleq \bigcup\nolimits_{n\in\mathbb{G}} \left(\mathbb{F}_r + nM^r\right), r \in \mathbb{N}^+, \end{aligned} \tag{12}$$

where $M \triangleq |\mathbb{U}|$ and r is the fractal order belonging to the set of positive integers $\mathbb{N}^+$. Here $\mathbb{U}$ is the longest central ULA segment in the second-order difference co-array of the generator $\mathbb{G}$, and $|\cdot|$ returns the cardinality of the input set. It has been shown in [3] that the second-order difference co-array of $\mathbb{F}_r$ contains consecutive lags in $\mathbb{U}_{2(\mathbb{F}_r)} = [-\frac{M^r-1}{2}, \frac{M^r-1}{2}]$.

The connection between the maximum consecutive lag $\max(\mathbb{U}_{2(\mathbb{F}_r)})$ and the physical sensors in $\mathbb{F}_r$ is a topic of interest. Which pair of physical sensors produces $\max(\mathbb{U}_{2(\mathbb{F}_r)})$? What is the relationship between this sensor pair and the elements in the generator array $\mathbb{G}$? The answers are given in *Lemma 1*. Furthermore, as will be introduced in the next subsection, $\mathbb{F}_r$ is part of the sparse array based on the $2q$th-order difference co-array generated from $\mathbb{G}$, and this lemma is beneficial for improvement of DOFs via sensor sharing between adjacent subarrays under design.

Lemma 1: For the SO-Fractal $\mathbb{F}_r$ $(r \geq 1)$ generated from $\mathbb{G}$, the largest consecutive lag guaranteed in its second-order difference co-array is constructed by

$$f_{r(i)} - f_{r(j)} = \max(\mathbb{U}_{2(\mathbb{F}_r)}) = \tfrac{M^r-1}{2}, \tag{13}$$

and the sensor pair $(f_{r(i)}, f_{r(j)}) \in \mathbb{F}_r^2$ can be expressed as

$$f_{r(i)} = \sum\nolimits_{k=0}^{r-1} g_i M^k,\ f_{r(j)} = \sum\nolimits_{k=0}^{r-1} g_j M^k,\ r \in \mathbb{N}^+, \tag{14}$$

where the specific sensor pair $(g_i, g_j) \in \mathbb{G}^2$ satisfying $g_i - g_j = \max(\mathbb{U}) = \frac{M-1}{2}$. Note that (g_i, g_j) is one potential pair to produce the largest consecutive lag. In particular, if the second-order difference co-array of $\mathbb{G}$ is hole-free, then $g_i = \max(\mathbb{G})$ and $g_j = \min(\mathbb{G})$.

Proof: To begin, we prove that sensor positions $f_{r(j)}$ and $f_{r(i)}$ in (14) are elements in $\mathbb{F}_r$ by mathematical induction. For $r = 1$, one has $(f_{1(i)}, f_{1(j)}) = (g_i, g_j) \in \mathbb{G}^2$ and $\mathbb{G} = \mathbb{F}_1$, yielding $f_{1(i)} - f_{1(j)} = \frac{M-1}{2}$ and $(f_{1(i)}, f_{1(j)}) \in \mathbb{F}_1^2$.

For $r = k$, assume that $(f_{k(i)}, f_{k(j)}) \in \mathbb{F}_k^2$. Then, for $r = k+1$, the definition of $\mathbb{F}_{k+1}$ is

$$\mathbb{F}_{k+1} = \left\{ l + nM^k \mid l \in \mathbb{F}_k,\ n \in \mathbb{G} \right\}. \tag{15}$$

Since $(f_{k(i)}, f_{k(j)}) \in \mathbb{F}_k^2$ and $(g_i, g_j) \in \mathbb{G}^2$, one obtains $f_{k+1(i)} = f_{k(i)} + g_i M^k$, $f_{k+1(j)} = f_{k(j)} + g_j M^k$, and $(f_{k+1(i)}, f_{k+1(j)}) \in \mathbb{F}_{k+1}^2$, which completes the induction. The difference between $f_{r(i)}$ and $f_{r(j)}$ is

$$\begin{aligned} f_{r(i)} - f_{r(j)} &= \sum\nolimits_{k=0}^{r-1} (g_i - g_j) M^k \\ &= \tfrac{M-1}{2} \cdot \tfrac{1-M^r}{1-M} = \tfrac{M^r-1}{2}, \end{aligned} \tag{16}$$

where $\max(\mathbb{U}_{2(\mathbb{F}_r)}) = \frac{M^r-1}{2}$ is the largest consecutive lag guaranteed in the difference co-array of $\mathbb{F}_r$. ∎

Several examples are given in Fig. 1 to demonstrate the SO-Fractal structure and *Lemma 1*. The nested array $\{0, 1, 2, 5\}$ and expanded coprime array $\{0, 2, 3, 4, 6\}$ are chosen as generators. The nested array provides a maximum consecutive lag of 5 in its hole-free second-order difference co-array. The expanded coprime array provides a maximum consecutive lag of 4 and has holes in its virtual array. The SO-Fractal ($r = 2$) is generated from the generators with $M = |\mathbb{U}| = 2 \cdot 5 + 1 = 11$ or $M = 2 \cdot 4 + 1 = 9$. For the nested array without holes in its second-order difference co-array, the maximum consecutive lag 5 is obtained by the difference between the rightmost sensor and the leftmost sensor, i.e., $g_i - g_j = 5 - 0 = \max(\mathbb{U}) = 5$. As shown in Fig. 1(d), the largest virtual sensor (in the consecutive difference co-array lags) provided by the SO-Fractal generated from the nested array is obtained by $f_{2(i)} - f_{2(j)} = \sum_{k=0}^{1} (g_i - g_j) M^k = 60$. For the fractal array generated by the expanded coprime array, it is similar to the previous one, as verified in Fig. 1(h).

B. Fractal Array Exploiting 2qth-Order Difference Co-Array

We now introduce fractal arrays based on the $2q$th-order difference co-array, referred to as $2q$th-O-Fractal.

Definition 4: The $2q$th-O-Fractal $\mathbb{E}_r^{2q} = \bigcup_{l=1}^{q} \mathbb{E}_{r(l)}$ consists of q subarrays, i.e., $\mathbb{E}_{r(1)}, \mathbb{E}_{r(2)}, \cdots, \mathbb{E}_{r(q)}$, where

$$\mathbb{E}_{r(1)} \triangleq \bigcup_{n \in \mathbb{F}_r} (n \cdot T_1 + m_1) = \mathbb{F}_r, \tag{17}$$

$$\mathbb{E}_{r(2)} \triangleq \bigcup_{n \in \mathbb{E}_{r(1)}} (n \cdot T_2 + m_2), \tag{18}$$

$$\vdots$$

$$\mathbb{E}_{r(q)} \triangleq \bigcup_{n \in \mathbb{E}_{r(1)}} (n \cdot T_q + m_q). \tag{19}$$

The original SO-Fractal is denoted by $\mathbb{F}_r$. The expanding factor T_q and the offset term m_q are defined by recursive expressions, given by

$$\begin{aligned} &T_0 = 0,\ T_1 = 1, \\ &T_q = M^r \cdot T_{q-1} + (M^r - 1) \cdot T_{q-2},\ q \geq 2, \end{aligned} \tag{20}$$

$$\begin{aligned} &m_0 = 0,\ m_1 = 0, \\ &m_q = -f_{r(j)} \cdot T_q + f_{r(i)} \cdot T_{q-1} + m_{q-1},\ q \geq 2, \end{aligned} \tag{21}$$

where $(f_{r(i)}, f_{r(j)}) \in \mathbb{E}_{r(1)}^2$ is a sensor pair satisfying (13). The above across-order fractal design ensures structural similarity across cumulant order q (also considered as an across-order fractal factor). The sensor position set of the p-th level subarray $\mathbb{E}_{r(p)}$ ($1 \leq p \leq q$) with a fractal order r (inner-order fractal factor within the same cumulant order) is recursively defined as

$$\begin{aligned} \mathbb{E}_{0(p)} &= \{m_p\}, \\ \mathbb{E}_{r(p)} &= \bigcup_{n \in \mathbb{E}_{r(1)}} (n \cdot T_p + m_p) \\ &= \bigcup_{u \in \mathbb{G}} \left(\mathbb{E}_{r-1(1)} \cdot T_p + u \cdot T_p M^{r-1} + m_p \right), r \in \mathbb{N}^+, \end{aligned} \tag{22}$$

where $M \triangleq |\mathbb{U}|$ is the length of the central ULA segment in the second-order difference co-array of the generator $\mathbb{G}$.

In $2q$th-O-Fractal with q subarrays, the basic construction idea is that the p-th subarray is designed by dilating the first subarray with an expansion factor T_p ($2 \leq p \leq q$), followed by a shift with an offset m_p along the end-fire direction of the linear array. By doing so, 1) self-similarity is guaranteed among all subarrays; 2) a series of T_p ($2 \leq p \leq q$) is designed to ensure a large consecutive $2q$th-order difference co-array; 3) a series of specifically designed m_p enlarges the number of consecutive co-array lags by providing an additional virtual ULA segment, and reduces the sensor number by sharing one physical sensor between every two neighboring subarrays. Therefore, the expanding factor T_p is defined as the unit inter-element spacing of the p-th subarray, which is equal to the number of central ULA sensors in the $2(p-1)$-th order difference co-array of the $2(p-1)$th-O-Fractal $\mathbb{E}_r^{2(p-1)} = \bigcup_{h=1}^{p-1} \mathbb{E}_{r(h)}$, leading to a large consecutive difference co-array (see ϕ_2' in the proof of *Proposition 1*). The offset m_p in (21) is constructed based on the idea that a common physical sensor is shared by the subarrays with adjacent indices, i.e., $\mathbb{E}_{r(p-1)}$ and $\mathbb{E}_{r(p)}$, and an additional ULA set (see ϕ_3 in the proof of *Proposition 1*) can be obtained to increase uDOFs by optimizing this relationship between m_p and m_{p+1}. As a result, more uDOFs can be provided with a fixed number of physical sensors. Detailed derivations of (20) and (21) are given in the proof of *Proposition 1*.

Proposition 1: For the $2q$th-O-Fractal $\mathbb{E}_r^{2q} = \bigcup_{l=1}^{q} \mathbb{E}_{r(l)}$, its $2q$th-order difference co-array $\mathbb{D}_{2q}$ has at least T_{q+1} consecutive co-array lags ranging from $-\frac{T_{q+1}-1}{2}$ to $\frac{T_{q+1}-1}{2}$, expressed as

$$\mathbb{D}_{2q} \supseteq \mathbb{U}_{2q}' = \left[-\tfrac{T_{q+1}-1}{2}, \tfrac{T_{q+1}-1}{2} \right],\ q \geq 1. \tag{23}$$

Proof: See Appendix A. ∎

Based on (21), we verify the sensor sharing strategy between every two adjacent subarrays. For the p-th and $(p-1)$-th subarrays ($2 \leq p \leq q$) where

$$\begin{aligned} \mathbb{E}_{r(p)} &= \{n_1 \cdot T_p + m_p \mid n_1 \in \mathbb{E}_{r(1)}\}, \\ \mathbb{E}_{r(p-1)} &= \{n_2 \cdot T_{p-1} + m_{p-1} \mid n_2 \in \mathbb{E}_{r(1)}\}, \end{aligned} \tag{24}$$

set $n_1 = f_{r(j)}$, $n_2 = f_{r(i)}$, and one gets

$$\begin{aligned} &f_{r(j)} \cdot T_p + m_p \in \mathbb{E}_{r(p)}, \\ &f_{r(i)} \cdot T_{p-1} + m_{p-1} \in \mathbb{E}_{r(p-1)}. \end{aligned} \tag{25}$$

According to (21), $f_{r(j)} \cdot T_p + m_p = f_{r(i)} \cdot T_{p-1} + m_{p-1}$, indicating that the sensor at $f_{r(j)} \cdot T_p + m_p$ is shared by $\mathbb{E}_{r(p)}$ and $\mathbb{E}_{r(p-1)}$. As mentioned earlier, sharing a sensor reduces the number of physical sensors, and an additional ULA set (see

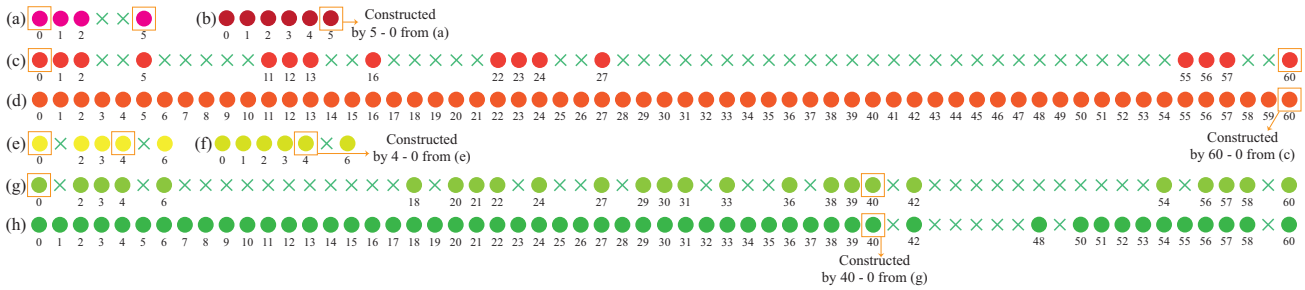

Fig. 1. Examples of SO-Fractal arrays and their difference co-arrays (non-negative part only): (a) nested array (as generator), (b) the second-order difference co-array of the nested array, (c) SO-Fractal ($r = 2$) generated from the nested array, (d) the second-order difference co-array of the SO-Fractal generated from the nested array, (e) expanded coprime array (as generator), (f) the second-order difference co-array of the expanded coprime array, (g) SO-Fractal ($r = 2$) generated from the expanded coprime array, (h) the second-order difference co-array of the SO-Fractal generated from the expanded coprime array.

ϕ_3 in the proof of *Proposition 1*) can be obtained to increase the number of consecutive co-array lags.

C. Examples

We give an example to illustrate how a simple generator is gradually expanded to a fractal array based on high-order cumulants. A MRA $\{0, 1, 3\}$ (see Fig. 2(a)) is chosen as the generator, and its second-order difference co-array is $\{-3, -2, -1, 0, 1, 2, 3\}$ with $M = 7$. From (12), the SO-Fractal $\mathbb{F}_2 = \mathbb{E}_{2(1)}$ (see Fig. 2(c)) is generated from $\mathbb{G} = \{0, 1, 3\}$ with the fractal order $r = 2$, and its second-order difference co-array contains continuous virtual sensors from -24 to 24. Therefore, the expanding factor of the second-level subarray of the 4th-O-Fractal is $T_2 = |\{-24, -23, \cdots, 23, 24\}| = 7^2 \cdot 1 + (7^2 - 1) \cdot 0 = 49$. By setting the offset term $m_2 = -0 \cdot 49 + 24 \cdot 1 + 0 = 24$, the physical sensor at 24 is shared by the first subarray and the second subarray as shown in Fig. 2(e).

IV. Properties of $2q$th-O-Fractal

For the proposed $2q$th-O-Fractal with closed-form sensor positions, the $2q$th-O-Fractal of large consecutive difference co-array (*Criterion 1*) and hole-free difference co-array (*Criterion 3*) are now discussed.

A. Analysis of Consecutive $2q$th-Order Difference Co-Array

We first analyze the $2q$th-order difference co-array of the $2q$th-O-Fractal. Based on *Proposition 1*, and the following corollary related to the consecutive co-array segment can be derived.

Corollary 1: Consider a generator array $\mathbb{G}$ with L sensors whose second-order difference co-array satisfies $|\mathbb{U}| = M = \mathcal{O}(L^2)$. Let $\mathbb{E}_r^{2q} = \cup_{l=1}^{q} \mathbb{E}_{r(l)}$ denote the $2q$th-O-Fractal with N sensors created by $\mathbb{G}$. The number of consecutive lags in its $2q$th-order difference co-array is

$$|\mathbb{U}_{2q}| = \mathcal{O}(N^{2q}), \tag{26}$$

where $N \leq qL^r - q + 1$.

Proof: We first focus on the number of physical sensors in $2q$th-O-Fractal. According to Theorem 2 in [3], the number of sensors in the first subarray $\mathbb{E}_{r(1)}$ satisfies $N_1 \leq L^r$. As we have seen, a common sensor is shared by every two adjacent subarrays, and thus the number of sensors in $2q$th-O-Fractal becomes

$$N = qN_1 - q + 1 \leq qL^r - q + 1. \tag{27}$$

In addition, if the generator $\mathbb{G}$ has hole-free second-order difference co-array, then $N = qL^r - q + 1$ is achieved.

Next, we consider the number of consecutive lags provided by $2q$th-O-Fractal. It is concluded in *Proposition* 1 that $|\mathbb{U}_{2q}| \geq T_{q+1}$ $(q \geq 1)$. We use mathematical induction to prove that $T_{q+1} = \mathcal{O}_c(c_{t(q)} M^{rq})$ $(q \geq 1)$ and the coefficient of highest-order term (denoted by $c_{t(q)}$) is 1. The notation $\mathcal{O}_c(g(N))$ indicates $g(N)$ can be achieved asymptotically when N tends to infinity with the argument $g(N)$ as the highest-order term including coefficient, and $f(N) = \mathcal{O}_c(g(N))$ means $\lim_{N\to\infty} \frac{f(N)}{g(N)} = 1$.

For $q = 1$ and $q = 2$, it is obvious that $T_2 = M^r = \mathcal{O}_c(c_{t(1)} M^r)$ with $c_{t1} = 1$ and $T_3 = M^{2r} + M^r - 1 = \mathcal{O}_c(c_{t(2)} M^{2r})$ with $c_{t(2)} = 1$. Assume that $T_k = \mathcal{O}_c(c_{t(k-1)} M^{r(k-1)})$ with $c_{t(k-1)} = 1$ for $q = k - 1$ and $T_{k+1} = \mathcal{O}_c(c_{t(k)} M^{r(k)})$ with $c_{t(k)} = 1$ for $q = k$. Then for $q = k + 1$,

$$\begin{aligned} T_{k+2} &= M^r \cdot T_{k+1} + (M^r - 1) \cdot T_k \\ &= \mathcal{O}_c(c_{t(k)} M^{r(k+1)} + c_{t(k-1)} M^{rk} - c_{t(k-1)} M^{r(k-1)}). \end{aligned} \tag{28}$$

Extracting the highest-order term (with degree $r(k + 1)$) of T_{k+2}, we obtain

$$T_{k+2} = \mathcal{O}_c(c_{t(k+1)} M^{r(k+1)}) = \mathcal{O}_c(M^{r(k+1)}). \tag{29}$$

Therefore, we conclude that

$$\begin{aligned} T_{q+1} &= \mathcal{O}_c(c_{t(q)} M^{rq}),\ q \geq 1 \\ c_{t(q)} &= 1. \end{aligned} \tag{30}$$

Since $M = \mathcal{O}(L^2)$ and $N \leq qL^r - q + 1 = \mathcal{O}(L^r)$, we have

$$M^r = \mathcal{O}(N^2). \tag{31}$$

Therefore, the number of consecutive $2q$th-order difference co-array lags provided by $2q$th-O-Fractal satisfies

$$|\mathbb{U}_{2q}| \geq T_{q+1} = \mathcal{O}(M^{rq}) = \mathcal{O}(N^{2q}). \tag{32}$$

Since no array can have more than $\mathcal{O}(N^{2q})$ elements in its $2q$th-order difference co-array according to *Definition 1*, we

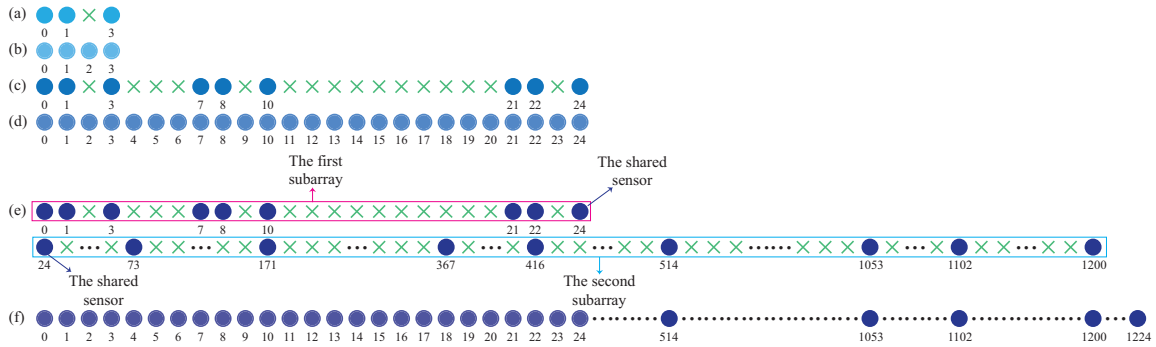

Fig. 2. An example for the process from a generator array to the 4th-O-Fractal, (a) generator array, (b) the second-order difference co-array of the generator array (non-negative part only), (c) SO-Fractal with fractal order $r = 2$, (d) the second-order difference co-array of the SO-Fractal (non-negative part only), (e) 4th-O-Fractal with fractal order $r = 2$, (f) the fourth-order difference co-array of the 4th-O-Fractal (which has holes and only the non-negative and consecutive part is shown here).

have $|\mathbb{U}_{2q}| \leq \mathcal{O}(N^{2q})$. In conclusion, $|\mathbb{U}_{2q}| = \mathcal{O}(N^{2q})$ is derived, which completes the proof. ■

According to (32) in *Corollary 1*, $\mathcal{O}(N^{2q})$ uDOFs (consecutive $2q$th-order difference co-array lags) can be provided by the proposed $2q$th-O-Fractal, which is significantly larger than $\mathcal{O}(N^2)$ provided by the original fractal array or other structures exploiting the second-order difference co-array. Furthermore, for an example with INA [12] as the generator, we can prove that the associated $2q$th-O-Fractal provides more uDOFs than existing structures (SE-$2q$L-NA [9] and $2q$L-NA [8]) based on the $2q$th-order difference co-array, as shown in the following proposition. The INA with $N_G = N_1^{'} + N_2^{'} + 1$ ($N_G > 5$) physical sensors is defined as

$$\begin{aligned}
&\mathbb{G}^{'} = \mathbb{G}_1^{'} \cup \mathbb{G}_2^{'} \cup \mathbb{G}_3^{'}, \qquad \mathbb{G}_1^{'} = [0, N_1^{'} - 1], \\
&\mathbb{G}_2^{'} = \{n \cdot (N_1^{'} + 2) + N_1^{'} \mid n \in [0, N_2^{'} - 1]\}, \\
&\mathbb{G}_3^{'} = \{N_1^{'} N_2^{'} + N_1^{'} + 2N_2^{'} - 1\},
\end{aligned} \tag{33}$$

where $\left(N_1^{'}, N_2^{'}\right) = \left(\frac{N_G}{2} - 1, \frac{N_G}{2}\right)$ if N_G is even, or $\left(N_1^{'}, N_2^{'}\right) = \left(\frac{N_G-1}{2} - 1, \frac{N_G+1}{2}\right)$ if N_G is odd [12], [14].

Proposition 2: For the $2q$th-O-Fractal $\mathbb{E}_1^{2q} = \cup_{l=1}^{q}(\mathbb{E}_{1(l)})$ ($q \geq 2$) generated by $\mathbb{G}^{'}$, the number of consecutive lags provided by its $2q$th-order difference co-array exceeds those of SE-$2q$L-NA [9] and $2q$L-NA [8] under the same number of physical sensors.

Proof: Note that $|\mathbb{E}_1^{2q}| = qN_G - q + 1$. For even N_G, one has $|\mathbb{E}_1^{2q}| = qN_G - q + 1 = 2q(N_1^{'} + 1) - q + 1$. Then, for the SE-$2q$L-NA with $2q(N_1^{'} + 1) - q + 1 = \sum_{m=1}^{2q}(N_m - 1) + 2$ physical sensors, set $(N_1, \cdots, N_{q-1}, N_q, \cdots, N_{2q}) = (N_1^{'} + 2, \cdots, N_1^{'} + 2, N_1^{'} + 1, \cdots, N_1^{'} + 1)$, which implies the optimal allocation strategy is adopted and the number of consecutive lags achieved is $L_q = 2^q(N_1^{'}+2)^{q-1}(N_1^{'}+1)^{q+1} + 2^{q-1}(N_1^{'}+2)^{q-1}(N_1^{'}+1)^{q-1} + 1$. For the $2q$th-O-Fractal, $T_2 = M^r = 2(N_1^{'}+1)^2 + 4(N_1^{'}+1) - 3$ according to the number of DOFs obtained by the second-order difference co-array of INA [12].

Next, we prove that $T_{q+1} > L_q$ is true for $q \geq 2$ by mathematical induction. For $q = 2$ and $q = 3$, one obtains

$$T_3 - L_2 = 2N_1^{'}(6N_1^{'2} + 20N_1^{'} + 11) - 2 > 0, \tag{34}$$

$$\begin{aligned}
T_4 - L_3 = 2N_1^{'}\{N_1^{'}[4N_1^{'}(N_1^{'}(4N_1^{'} + 27) + 61) \\
+ 199] + 44\} - 10 > 0.
\end{aligned} \tag{35}$$

Assume that $T_{k+1} > L_k$ and also $T_{k+2} > L_{k+1}$ for $q = k$ and $q = k + 1$. Then, for $q = k + 2$,

$$\begin{aligned}
&T_{k+3} - L_{k+2} = M^r T_{k+2} + (M^r - 1)T_{k+1} - L_{k+2} \\
&> M^r L_{k+1} + (M^r - 1)L_k - L_{k+2} \\
&= 2^k[2N_1^{'}(N_1^{'} + 2) + 3]\{N_1^{'}[2N_1^{'}(N_1^{'} + 3) + 5] - 1\} \\
&\quad (N_1^{'} + 1)^{k-1}(N_1^{'} + 2)^{k-1} + 4N_1^{'}(N_1^{'} + 4) + 4 > 0,
\end{aligned} \tag{36}$$

which completes the proof of $T_{q+1} > L_q$ ($q \geq 2$ and N_G is even).

For odd N_G, one has $|\mathbb{E}_1^{2q}| = qN_G - q + 1 = q(2N_1^{'} + 3) - q + 1$, and $T_2 = M^r = (2N_1^{'} + 3)^2/2 + 2(2N_1^{'} + 3) - 7/2$ [12], [14]. Then, the sensors of SE-$2q$L-NA are allocated by $(N_1, \cdots, N_{2q-1}, N_{2q}) = (N_1^{'}+2, \cdots, N_1^{'}+2, N_1^{'}+1)$ according to the optimization strategy, and the number of consecutive lags is $L_q = 2^q(N_1^{'}+2)^{2q-1}(N_1^{'}+1) + 2^{q-1}(N_1^{'}+2)^{2q-2} + 1$. Similarly, one can prove $T_{q+1} > L_q$ for $q \geq 2$ by mathematical induction, and the details are omitted.

Due to Corollary 4 in [9], an optimized SE-$2q$L-NA always provides more consecutive lags than any configurations of $2q$L-NA with the same number of sensors with $N_{2q} > 2$. Therefore, the number of consecutive $2q$th-order difference co-array lags provided by the proposed $2q$th-O-Fractal is greater than those provided by SE-$2q$L-NA and $2q$L-NA. ■

In *Proposition 2*, we prove that the number of uDOFs provided by $2q$th-O-Fractal with INA ($N_G > 5$) as the generator array exceeds those of SE-$2q$L-NA and $2q$L-NA, where the number of physical sensors covers a wide range including both small and large numbers. However, the asymptotic number of uDOFs when N tends to infinity and its relationship with q are of great interest, which depends on the coefficient of the highest-order term. Assume that $\mathcal{O}_c(C_F N^{2q})$ uDOFs can be provided by the $2q$th-O-Fractal. To further compare the coefficient C_F with those of existing structures and explore its relationship with cumulant order q, *Proposition 3* is given below. The IMISC structure with 6 subarrays based on the second-order difference co-array is chosen as the generator

array, and its sensor position set is defined as [15]

$$\begin{aligned}
&\mathbb{G}_{\text{IM}} = \mathbb{G}_{\text{IM1}} \cup \mathbb{G}_{\text{IM2}} \cup \mathbb{G}_{\text{IM3}} \cup \mathbb{G}_{\text{IM4}} \cup \mathbb{G}_{\text{IM5}} \cup \mathbb{G}_{\text{IM6}}, \qquad (37)\\
&\mathbb{G}_{\text{IM1}} = \{2g_1 \mid g_1 \in [0, \tfrac{N_M}{4} - 1]\},\\
&\mathbb{G}_{\text{IM2}} = \{g_2 + \tfrac{N_M}{2} - 1 \mid g_2 \in [0, 1]\},\\
&\mathbb{G}_{\text{IM3}} = \{\tfrac{N_M-2}{2} g_3 + N_M - 2 \mid g_3 \in [0, \tfrac{N_M}{4} - 2]\},\\
&\mathbb{G}_{\text{IM4}} = \{N_M g_4 + \tfrac{N_M^2+6N_M}{8} \mid g_4 \in [0, N_G - N_M - 1]\},\\
&\mathbb{G}_{\text{IM5}} = \{\tfrac{N_M+2}{2} g_5 + N_M N_G - \tfrac{7N_M^2-2N_M-8}{8} \mid\\
&\qquad g_5 \in [0, \tfrac{N_M}{4} - 2]\},\\
&\mathbb{G}_{\text{IM6}} = \{2g_6 + N_M N_G - \tfrac{3N_M^2+2N_M-4}{4} \mid g_6 \in [0, \tfrac{N_M}{4} - 1]\},
\end{aligned}$$

where $N_G > 9$ is the sensor number, and $N_M = 4\left\lfloor \frac{N_G+2}{6} \right\rfloor$.

Proposition 3: The number of consecutive co-array lags T_{q+1} provided by $2q$th-O-Fractal with generator $\mathbb{G}_{\text{IM}}$ is given by

$$T_{q+1} = \mathcal{O}_c(C_F N^{2q}) = \mathcal{O}_c(\frac{2^q}{q^{2q}3^q} N^{2q}), \quad q \geq 1, \qquad (38)$$

where N is the physical sensor number. Consider $2q$L-NA [8] and SE-$2q$L-NA [9] with the same sensor number. The number of consecutive co-array lags in $2q$L-NA and SE-$2q$L-NA is denoted as $L_q = \mathcal{O}_c(C_L N^{2q})$ and $S_q = \mathcal{O}_c(C_S N^{2q})$, respectively. We have

$$\lim_{N\to+\infty} \frac{T_{q+1}}{L_q} = \frac{C_F}{C_L} = \frac{8^q}{2 \cdot 3^q} > 1, \quad q \geq 2, \qquad (39)$$

$$\lim_{N\to+\infty} \frac{T_{q+1}}{S_q} = \frac{C_F}{C_S} = \frac{4^q}{3^q} > 1, \quad q \geq 2. \qquad (40)$$

Proof: In *Corollary 1*, we have proven that $T_{q+1} = \mathcal{O}_c(c_{t(q)} M^{rq})$ ($q \geq 1$) and the coefficient of the highest-order term $c_{t(q)} = 1$.

Choosing IMISC as the generator, the parameter M^r of the $2q$th-O-Fractal $\mathbb{E}_r^{2q}$ for $r = 1$ satisfies

$$M^r = \frac{2N_G^2}{3} - \frac{2N_G}{3} + c_{t0}, \qquad (41)$$

where c_{t0} is a constant with [15]

$$c_{t0} = \begin{cases} -1, & \mod (N_G, 6) = 3 \text{ or } 4,\\ \frac{5}{3}, & \mod (N_G, 6) = 2 \text{ or } 5,\\ 3, & \mod (N_G, 6) = 0 \text{ or } 1. \end{cases} \qquad (42)$$

According to $N_G = \frac{N+q-1}{q}$ and (41), we obtain

$$M^r = \frac{2N^2}{3q^2} + N\left(\frac{2}{3q} - \frac{4}{3q^2}\right) + \frac{2}{3q^2} - \frac{2}{3q} + c_{t0}. \qquad (43)$$

Combining (30) and (43) leads to

$$T_{q+1} = \mathcal{O}_c(c_{t(q)} M^{rq}) = \mathcal{O}_c(\frac{2^q}{3^q q^{2q}} N^{2q}) = \mathcal{O}_c(C_F N^{2q}). \qquad (44)$$

For $2q$L-NA and SE-$2q$L-NA, the sensor number of the i-th subarray is $N_i = \frac{N_t+2q-1}{2q}$. N_i follows the optimal allocation strategy achieving maximum number of consecutive co-array lags without constraining N_i to be an integer [8], [9]. As a result, the number of consecutive lags in $2q$L-NA and SE-$2q$L-NA is respectively [8], [9]

$$L_q = 2^{2-2q}\left(\tfrac{N+2q-1}{q}\right)^{2q-1}\left(\tfrac{N+2q-1}{2q} + 1\right) - 1, \ q \geq 2, \qquad (45)$$

$$S_q = 2^{-q}\left(\tfrac{N+2q-1}{q}\right)^{2q} + 2^{1-q}\left(\tfrac{N+2q-1}{q}\right)^{2q-2} + 1, \ q \geq 2. \qquad (46)$$

Focusing on the coefficient of the highest-order term (i.e., N^{2q}), we obtain

$$L_q = \mathcal{O}_c(C_L N^{2q}) = \mathcal{O}_c(\frac{1}{2^{2q-1} q^{2q}} N^{2q}), \qquad (47)$$

$$S_q = \mathcal{O}_c(C_S N^{2q}) = \mathcal{O}_c(\frac{1}{2^q q^{2q}} N^{2q}). \qquad (48)$$

Combining (47), (48) and (44), it can be derived that

$$\lim_{N\to+\infty} \frac{T_{q+1}}{L_q} = \frac{C_F}{C_L} = \frac{8^q}{2 \cdot 3^q} > 1, \quad q \geq 2, \qquad (49)$$

$$\lim_{N\to+\infty} \frac{T_{q+1}}{S_q} = \frac{C_F}{C_S} = \frac{4^q}{3^q} > 1, \quad q \geq 2. \qquad (50)$$

Therefore, $C_F > C_L$ and $C_F > C_S$. For a large sensor number N, the number of consecutive co-array lags provided by the proposed structure is approximately $\frac{8^q}{2 \cdot 3^q}$ times that of $2q$L-NA and $\frac{4^q}{3^q}$ times that of SE-$2q$L-NA. The ratio of uDOFs number provided by $2q$th-O-Fractal to that provided by existing structures increases exponentially with cumulant order q. ∎

Recently, a tight upper bound $\kappa_4(N)$ on the number of DOFs for $q = 2$ was derived in [61], given by

$$\kappa_4(N) = \frac{N^4}{4} - \frac{N^3}{2} + \frac{7N^2}{4} - \frac{3N}{2} + 1 = \mathcal{O}_c(\frac{N^4}{4}), \qquad (51)$$

where the notation $\mathcal{O}_c(g(N))$ indicates $g(N)$ can be achieved asymptotically when N tends to infinity with the argument $g(N)$ as the highest-order term including coefficient, and $f(N) = \mathcal{O}_c(g(N))$ means $\lim_{N\to\infty} \frac{f(N)}{g(N)} = 1$. For a sufficiently large N, we have $\lim_{N\to\infty} \kappa_4(N) = \frac{N^4}{4}$.

Derivation of a tight upper bound on the number of DOFs for any q is a challenging problem due to the extremely large number of co-array elements (more complicated cases similar to those in [61] should be considered) and also space limit. In *Proposition 3*, we focus on the coefficient of highest-order term, indicating that the asymptotic number of uDOFs of the proposed structure is larger than those of existing structures when the number of sensors N tends to infinity. Therefore, we study the asymptotic upper bound on the number of DOFs when N tends to infinity instead to further verify the results in *Proposition 3*, and this bound can also be considered as a loose upper bound on the number of uDOFs.

Recall the definition of the $2q$th-order difference co-array, i.e., $\mathbb{D}_{2q} = \left\{ \sum_{k=1}^{q} \mu_k - \sum_{l=q+1}^{2q} \mu_l \mid \mu_k, \ \mu_l \in \mathbb{A} \right\}$. $\binom{N}{q} = \frac{N!}{q!(N-q)!}$ returns the number of combinations of choosing q distinct elements from N, with $N!$ being the factorial of N. Similar to the analysis in [61] and [43], only for the case where $\mu_1, \mu_2, \cdots, \mu_{2q}$ are all distinct, the number of virtual elements associated reaches $\mathcal{O}(N^{2q})$. For all other cases, the

highest-order is smaller than $2q$. By picking q non-ordered distinct numbers from N physical sensors to form $\sum_{k=1}^{q}\mu_k$, followed by picking another q non-ordered distinct numbers from the rest $N-q$ sensors to generate $-\sum_{l=q+1}^{2q}\mu_l$, the number of combinations is

$$F_{2q}=\binom{N}{q}\cdot\binom{N-q}{q}=\frac{N!}{q!q!(N-2q)!}=\mathcal{O}_c(\frac{N^{2q}}{q!q!}). \tag{52}$$

Therefore, when N tends to infinity, the number of DOFs (unique difference co-array elements) should be smaller than $\mathcal{O}_c(\frac{N^{2q}}{q!q!})$, with $\frac{N^{2q}}{q!q!}$ being the asymptotic upper bound. Simply, we have

$$C_{\text{ub}(2q)}=\frac{1}{q!q!}\geq\frac{1}{q^q q^q}=\frac{1}{q^{2q}}. \tag{53}$$

Let C_F, C_L, and C_S represent the coefficients of the highest-order term N^{2q} of the number of uDOFs provided by $2q$th-O-Fractal, $2q$L-NA, and SE-$2q$L-NA, respectively. As proved in *Proposition 3*, we have

$$C_F=\frac{2^q}{3^q q^{2q}},\ C_L=\frac{1}{2^{2q-1}q^{2q}},\ C_S=\frac{1}{2^q q^{2q}}. \tag{54}$$

All of them are smaller than $C_{\text{ub}(2q)}$ (the coefficient of the upper bound). Furthermore, the asymptotic upper bound $\frac{N^{2q}}{q!q!}$ indicates that it decreases rapidly with the increase of q, clarifying potential margin for further improvement.

B. Discussion on the Hole-Free Property for $q=2$

Optimizing the sparse array configuration with a large and also hole-free difference co-array (*Criteria 1* and *3*) is a difficult problem. For $q>2$, the hole-free property has not been considered in the literature to the best of our knowledge. The hole-free property requires that the largest element $q[\max(\mathbb{A})-\min(\mathbb{A})]$ in the $2q$th-order difference co-array (according to *Definition 1*) must belong to the central virtual ULA segment. This requirement is in conflict with the criterion of achieving a large consecutive difference co-array.

In previous works, the array structures designed for the $2q$th-order cumulants only achieve hole-free in the case of $q=2$, and provide $\mathcal{O}(N^{3.17})$ DOFs at most. Several sparse arrays providing hole-free fourth-order difference co-array include 2L-FO-NA [49], CNA [50], GCNA [51], and E-FO-Cantor [52]. These structures are not flexible, and the other criteria are not considered in the design process. Therefore, we focus on the most common special case of $q=2$, and consider the selection of the generator array based on which the generated 4th-O-Fractal provides hole-free fourth-order difference co-array.

The hole-free property of the generator $\mathbb{G}$ is inherited by the corresponding SO-Fractal for $q=1$ [37]. However, the generator $\mathbb{G}$ has a hole-free second-order difference co-array, which is not a sufficient condition for 4th-O-Fractal to achieve a hole-free fourth-order difference co-array. A stronger constraint on $\mathbb{G}$ is required to ensure the hole-free property for $q=2$. Before discussing this constraint in *Proposition 4*, *Lemma 2* is introduced first.

Lemma 2: Consider a generator array $\mathbb{G}$ with hole-free sum co-array $\mathbb{S}$ and second-order difference co-array $\mathbb{D}$. The sum co-array $\mathbb{S}_r$ of the associated $\mathbb{F}_r$ has $|\mathbb{S}_r|=M^r$ consecutive lags with

$$\mathbb{S}_r=\left[\tfrac{2(M^r-1)\min(\mathbb{G})}{M-1},\ M^r+\tfrac{2(M^r-1)\min(\mathbb{G})}{M-1}-1\right].$$

Proof: Proved by mathematical induction. For $r=0$, one has $\mathbb{F}_0=\{0\}$ and $\mathbb{S}_0=\{0\}=[0,M^0-1]$, while for $r=1$, $\mathbb{F}_1=\mathbb{G}$ and $\mathbb{S}_1=\mathbb{S}=[2\min(\mathbb{G}),2\max(\mathbb{G})]$. Since $\mathbb{D}$ is hole-free and $|\mathbb{D}|=M$, one has $M=2\max(\mathbb{G})-2\min(\mathbb{G})+1$ and $\mathbb{S}_1=[2\min(\mathbb{G}),M+2\min(\mathbb{G})-1]$. For $r=k$, assume

$$\mathbb{S}_k=\left[\tfrac{2(M^k-1)\min(\mathbb{G})}{M-1},\ M^k+\tfrac{2(M^k-1)\min(\mathbb{G})}{M-1}-1\right]. \tag{55}$$

Then, for $r=k+1$,

$$\begin{aligned}\mathbb{S}_{k+1}&=\{\mu_1+\mu_2\mid\mu_1,\mu_2\in\mathbb{F}_{k+1}\}\\&=\{s+u\cdot M^k+(t+v\cdot M^k)\mid s,t\in\mathbb{F}_k,u,v\in\mathbb{G}\}\\&=\{(s+t)+(u+v)\cdot M^k\mid s,t\in\mathbb{F}_k,u,v\in\mathbb{G}\}\\&=\{p+q\cdot M^k\mid p\in\mathbb{S}_k,q\in\mathbb{S}_1\}.\end{aligned} \tag{56}$$

According to $\mathbb{S}_k$ with $|\mathbb{S}_k|=M^k$ in (55), $\mathbb{S}_{k+1}$ is hole-free and

$$\mathbb{S}_{k+1}=\left[\tfrac{2(M^{k+1}-1)\min(\mathbb{G})}{M-1},M^{k+1}+\tfrac{2(M^{k+1}-1)\min(\mathbb{G})}{M-1}-1\right],$$

which completes the proof. ∎

Proposition 4: A sufficient condition for the 4th-O-Fractal $\mathbb{E}_r^4$ to possess a hole-free fourth-order difference co-array $\mathbb{D}_4$ is that the associated generator array $\mathbb{G}$ has hole-free second-order difference co-array $\mathbb{D}$ and sum co-array $\mathbb{S}$. In this case, $\mathbb{D}_4$ can be expressed as

$$\mathbb{D}_4=\left[1-M^{2r},M^{2r}-1\right]. \tag{57}$$

Proof: From *Proposition 1*, one has

$$\mathbb{D}_4\supseteq\phi_4=\left[-\tfrac{T_3-1}{2},\tfrac{T_3-1}{2}\right]=\left[-\tfrac{M^{2r}+M^r-2}{2},\tfrac{M^{2r}+M^r-2}{2}\right].$$

Based on the given $\mathbb{G}$, construct a set $\phi_5\subseteq\mathbb{D}_4$, given by

$$\begin{aligned}\phi_5&=\{(\mu_1-\mu_2)-(\mu_3-\mu_4)|\mu_1,\mu_4\in\mathbb{E}_{r(2)},\mu_2,\mu_3\in\mathbb{E}_{r(1)}\}\\&=\{(\mu_1+\mu_4)-(\mu_2+\mu_3)|\mu_1,\mu_4\in\mathbb{E}_{r(2)},\mu_2,\mu_3\in\mathbb{E}_{r(1)}\}\\&=\{(s+t)\cdot T_2-(u+v)+2m_2\mid s,t,v,u\in\mathbb{F}_r\}\\&=\{(s+t)\cdot M^r-(u+v)+2m_2\mid s,t,v,u\in\mathbb{F}_r\}\\&=\{p\cdot M^r-q+2m_2\mid p,q\in\mathbb{S}_r\}.\end{aligned} \tag{58}$$

According to *Lemma 2*, one obtains

$$\begin{aligned}\phi_5=\Big[&2m_2+\tfrac{2(M^{2r}-2M^r+1)\min(\mathbb{G})}{M-1}-M^r+1,\\&2m_2+\tfrac{2(M^{2r}-2M^r+1)\min(\mathbb{G})}{M-1}+M^{2r}-M^r\Big].\end{aligned}$$

The offset term m_2 is

$$m_2=-f_{r(j)}\cdot M^r+f_{r(i)}=(g_i-g_jM^r)\cdot\tfrac{M^r-1}{M-1}. \tag{59}$$

Since $\mathbb{G}$ has hole-free second-order difference co-array, $g_i=\max(\mathbb{G})=\min(\mathbb{G})+\frac{M-1}{2}$ and $g_j=\min(\mathbb{G})$. Then, $2m_2$ can be represented as $M^r-1-\frac{2(M^{2r}-2M^r+1)\min(\mathbb{G})}{M-1}$, and thus

$$\phi_5=[0,M^{2r}-1]. \tag{60}$$

Similarly,

$$\begin{aligned}\phi_6 &= \{(\mu_1-\mu_2)-(\mu_3-\mu_4)|\mu_1,\mu_4\in\mathbb{E}_{r(1)},\mu_2,\mu_3\in\mathbb{E}_{r(2)}\}\\ &= [1-M^{2r},0]\subseteq\mathbb{D}_4. \end{aligned}\tag{61}$$

Note that the self-differences within subarrays are included in the set of cross-differences between subarrays, and therefore $\mathbb{D}_4=\phi_4\cup\phi_5\cup\phi_6$. The longest central ULA in $\mathbb{D}_4$ is $\phi_4\cup\phi_5\cup\phi_6$. As a result, the 4th-O-Fractal $\mathbb{E}_r^4$ has hole-free fourth-order difference co-array with

$$\mathbb{D}_4=[1-M^{2r},M^{2r}-1],\tag{62}$$

and the number of consecutive lags in the fourth-order difference co-array is $|\mathbb{D}_4|=2M^{2r}-1$. ■

According to *Proposition 4*, to ensure the hole-free property of $\mathbb{G}$ is inherited by the 4th-O-Fractal, both the second-order difference and sum co-arrays of $\mathbb{G}$ should be hole-free. The selection of an appropriate generator is a challenging problem. For example, the notable NA has contiguous second-order difference co-array, but its sum co-array has holes.

C. Examples of Appropriate Generator Arrays

We present several array structures meeting the mentioned constraint on the generator, including ULA, postage stamp bases [62], [63] extracted from number theory, general symmetric array [30], [64], and concatenated NA [64]. By choosing a proper generator, 4th-O-Fractal with N physical sensors can provide $\mathcal{O}(N^4)$ hole-free fourth-order difference co-array lags.

1) ULA: For a ULA, obviously its sum and difference co-arrays are hole-free, satisfying *Proposition 4*.

2) Extremal restricted additive 2-bases: The extremal restricted additive 2-bases comes from the postage stamp problem in number theory [62], [63], [65], [66].

For an extremal restricted additive 2-bases $\mathbb{A}_k=\{0<a_1<a_2<\cdots<a_k\}$, every integer in $[0,2a_k]$ is the sum of two elements in $\mathbb{A}_k$ [63], [66]. By regarding $\mathbb{A}_k$ as the set of sensor positions, its sum co-array $\mathbb{S}_A\triangleq\{\mu_1+\mu_2\mid\mu\in\mathbb{A}_k\}$ is hole-free. The algorithms in [63], [66] effectively reduce the feasible region for search and obtain $\mathbb{A}_k$ for $1\le k\le 47$. Furthermore, for each k, there is at least one $\mathbb{A}_k$ that is symmetric, i.e., $\mathbb{A}_k=a_k-\mathbb{A}_k$ [63], [66]. According to the definition of the extremal restricted additive 2-bases and the following proposition, the symmetric $\mathbb{A}_k$ ($k\le 47$) provided in [63], [66] can be employed as the generator.

Proposition 5: Consider an integer set $\mathbb{A}_k=\{a_0<a_1<\cdots<a_k\}$ representing the sensor positions of a symmetric array, where $\mathbb{A}_k=a_0+a_k-\mathbb{A}_k$. If the sum co-array (denoted by $\mathbb{S}_A$) of $\mathbb{A}_k$ is hole-free, then its second-order difference co-array $\mathbb{D}_A$ is also hole-free, and vice versa.

Proof: Due to the symmetric property of $\mathbb{A}_k$, the second-order difference co-array of $\mathbb{A}_k$ is

$$\begin{aligned}\mathbb{D}_A&=\{\mu_1-\mu_2\mid\mu_1,\mu_2\in\mathbb{A}_k\}\\ &=\{\mu_1-(a_0+a_k-\mu_3)\mid\mu_1,\mu_3\in\mathbb{A}_k\}\\ &=\{\mu_1+\mu_3-a_0-a_k\mid\mu_1,\mu_3\in\mathbb{A}_k\}.\end{aligned}\tag{63}$$

If the sum co-array $\mathbb{S}_A$ is hole-free, we simply have $\mathbb{S}_A=[2a_0,2a_k]$, and the following can be derived:

$$\begin{aligned}\mathbb{D}_A&=\{\mu_1+\mu_3-a_0-a_k\mid\mu_1,\mu_3\in\mathbb{A}_k\}\\ &=\{\mu_4-a_0-a_k\mid\mu_4\in\mathbb{S}_A\}=[a_0-a_k,a_k-a_0].\end{aligned}\tag{64}$$

As a result, the second-order difference co-array $\mathbb{D}_A$ is also hole-free.

Next, we consider the case where the second-order difference co-array $\mathbb{D}_A$ is hole-free. Since $\mathbb{D}_A=[a_0-a_k,a_k-a_0]$ is hole-free, we obtain

$$\begin{aligned}\mathbb{S}_A&=\{\mu_5+a_0+a_k-\mu_6\mid\mu_5,\mu_6\in\mathbb{A}_k\}\\ &=\{\mu_7+a_0+a_k\mid\mu_7\in\mathbb{D}_A\}=[2a_0,2a_k],\end{aligned}\tag{65}$$

which means that the sum co-array $\mathbb{S}_A$ is also hole-free. ■

The symmetric extremal restricted additive 2-bases $\mathbb{A}_k$ is a possible generator to ensure that hole-free property is inherited by the associated 4th-O-Fractal $\mathbb{E}_r^4$. Moreover, the definition of extremal restricted additive 2-bases implies that its redundancy is low. Utilizing this class of arrays as a generator leads to a large number of DOFs.

3) General symmetric array: Any linear array with hole-free second-order difference co-array is able to form a general symmetric array according to *Definition 5*.

Definition 5: The symmetric array $\mathbb{A}_{\text{sym}}$ is constructed from an original array $\mathbb{A}_1$ with $\mathbb{A}_{\text{sym}}\triangleq\mathbb{A}_1\cup\mathbb{A}_2$, where $\mathbb{A}_2\triangleq\{\max(\mathbb{A}_1)+\min(\mathbb{A}_1)-\mu\mid\mu\in\mathbb{A}_1\}$ is the reversed version of the original array $\mathbb{A}_1$ [30].

Proposition 6: Denote the second-order difference (sum) co-array of $\mathbb{A}_{\text{sym}}$ and $\mathbb{A}_1$ as $\mathbb{D}_{\text{sym}}$ ($\mathbb{S}_{\text{sym}}$) and $\mathbb{D}_1$ ($\mathbb{S}_1$), respectively. If $\mathbb{D}_1$ ($\mathbb{S}_1$) is hole-free, then $\mathbb{D}_{\text{sym}}$ ($\mathbb{S}_{\text{sym}}$) is also hole-free.

Proof: Since the maximum and minimum values in $\mathbb{A}_{\text{sym}}$ and $\mathbb{A}_1$ are the same, if $\mathbb{D}_1$ is hole-free, $\mathbb{D}_{\text{sym}}\subseteq\mathbb{D}_1$. According to the definition, we have $\mathbb{A}_{\text{sym}}\supseteq\mathbb{A}_1$ and $\mathbb{D}_{\text{sym}}\supseteq\mathbb{D}_1$. Therefore, $\mathbb{A}_1$ and $\mathbb{A}_{\text{sym}}$ share the same second-order difference co-array with $\mathbb{D}_{\text{sym}}=\mathbb{D}_1$, which means $\mathbb{D}_{\text{sym}}$ is also hole-free.

Similarly, if $\mathbb{S}_1$ is hole-free, $\mathbb{S}_{\text{sym}}$ is also hole-free, which completes the proof. ■

According to *Proposition 5* and *Proposition 6*, the general symmetric array satisfies the condition given in *Proposition 4*. Symmetric structures of this type greatly expand the optional range of generators, and the proposed 4th-O-Fractal offers hole-free fourth-order difference co-array with $\mathcal{O}(N^4)$ DOFs. Based on *Propositions 4*, *5*, and *6*, we have the following *Corollary 2*.

Corollary 2: Consider $\mathbb{A}_1$ having hole-free second-order difference co-array with $\mathcal{O}(N_1^2)$ DOFs, where $N_1=|\mathbb{A}_1|$. The symmetric array $\mathbb{A}_{\text{sym}}$ is constructed from $\mathbb{A}_1$. By setting the generator $\mathbb{G}=\mathbb{A}_{\text{sym}}$, the generated N-sensor 4th-O-Fractal has hole-free fourth-order difference co-array with $\mathcal{O}(N^4)$ DOFs.

Proof: The number of sensors in $\mathbb{A}_{\text{sym}}$ (*Definition 5*) is not greater than $2N_1-2$, since the maximum and minimum elements are shared by $\mathbb{A}_1$ and $\mathbb{A}_2$ at least. The number of DOFs provided by the second-order difference co-array of $\mathbb{A}_{\text{sym}}$ is $M_{\text{sym}}=\mathcal{O}(N_1^2)=\mathcal{O}(N_2^2)$, where N_2 represents the number of sensors in $\mathbb{A}_{\text{sym}}$. By choosing the array generator $\mathbb{G}=\mathbb{A}_{\text{sym}}$, the 4th-O-Fractal containing $N\le 2N_2^r-1$ sensors

has hole-free fourth-order difference co-array with $|\mathbb{D}_4|$ DOFs achieved. Since both the sum and difference co-arrays of $\mathbb{G}$ are hole-free, one has $M = 2\max(\mathbb{G}) - 2\min(\mathbb{G}) + 1 = \mathcal{O}(N_2^2)$, and $|\mathbb{D}_4| = 2M^{2r} - 1 = \mathcal{O}(N_2^{4r}) = \mathcal{O}(N^4)$ according to *Proposition 4*. ∎

4) Concatenated NA: Concatenated NA is proposed in active sensing applications exploiting sum co-arrays [64]. It is defined as follows.

Definition 6: The sensor position set of a concatenated NA is defined as $\mathbb{C}_{N_1,N_2} \triangleq \mathbb{C}_1 \cup \mathbb{C}_2 \cup \mathbb{C}_3$, where $\mathbb{C}_1 = [0, N_1 - 1]$, $\mathbb{C}_2 = \{\mu \cdot (N_1+1) + N_1 \mid \mu \in [0, N_2 - 1]\}$, $\mathbb{C}_3 = \{\mu + N_2(N_1 + 1) \mid \mu \in [0, N_1 - 1]\}$, N_1 and N_2 are non-negative integers.

We discuss the number of DOFs by giving the following corollary, which is related to *Proposition 4*.

Corollary 3: If the generator is chosen as $\mathbb{G} = \mathbb{C}_{N_1,N_2}$, the associated 4th-O-Fractal with N sensors has a hole-free fourth-order difference co-array with $\mathcal{O}(N^4)$ DOFs achieved.

Proof: The number of sensors in the generator is $L = |\mathbb{G}| = |\mathbb{C}_{N_1,N_2}|$, and $N \leq 2L^r - 1$. According to [64], both the sum and difference co-arrays are hole-free, and the number of DOFs offered by the second-order difference co-array of $\mathbb{C}_{N_1,N_2}$ is $M_{\text{cn}} = \mathcal{O}(L^2)$. Therefore, $M = M_{\text{cn}} = \mathcal{O}(L^2)$, and $|\mathbb{D}_4| = 2M^{2r} - 1 = \mathcal{O}(L^{4r}) = \mathcal{O}(N^4)$ according to *Proposition 4*. ∎

We have shown that for the special case of $q = 2$, *Criteria 1-3* can be satisfied. Other generalized properties in *Criteria 4-5* will be discussed in the companion paper of Part II [60].

V. Comparisons and Simulation Results

In this section, the superiority of the proposed design is verified in terms of estimation accuracy and resolution capability compared with existing structures.

A. Comparisons with Existing Structures Having Large $2q$th-Order Difference Co-Array

Two existing array structures, i.e., $2q$L-NA [8] and SE-$2q$L-NA [9], are designed to pursue large $2q$th-order difference co-array. The number of achievable consecutive $2q$th-order difference co-array lags are compared in Table I.

We first focus on the property of large consecutive difference co-array. MRA [10], ENA [13], INA [12], and IMISC [15], containing high uDOFs in their second-order difference co-arrays, are chosen as generators, and the properties of large consecutive difference co-array and closed-form sensor positions (*Criteria 1* and *2*) can be inherited by their associated $2q$th-O-Fractal. For $q = 2$ and $q = 3$, specific examples with details of generators, number of sensors, and fractal orders, etc., are listed in Tables II and III. Obviously, significantly increased consecutive co-array lags (equivalent to the uniform DOFs) have been achieved by our proposed structure $2q$th-O-Fractal compared with existing structures.

In the previous *Proposition 2*, we theoretically proved that the $2q$th-O-Fractal with INA as a generator can provide more consecutive lags than existing structures with the same number of sensors, which is consistent with the results in Tables II and III. *Proposition 3* is verified in Fig. 3, where IMISC is the generator for the $2q$th-O-Fractal. The number of consecutive co-array lags with respect to the sensor number for $q = 2$ is shown in Fig. 3(a), while the number of consecutive co-array lags versus the cumulant order q is given in Fig. 3(b). It can be seen clearly that the proposed $2q$th-O-Fractal always offers the largest number of consecutive lags among all structures.

TABLE I
Comparison of the Consecutive Lags for Different Array Structures Based on the $2q$th-order ($q \geq 2$) Difference Co-Array

Array Structures	Number of Physical Sensors*	Number of Consecutive Lags
$2q$L-NA	$N = \sum_{m=1}^{2q}(N_m - 1) + 1$	$L_q = \mathcal{O}_c(\frac{1}{2^{2q-1}q^{2q}}N^{2q})^\dagger$
SE-$2q$L-NA	$N = \sum_{m=1}^{2q}(N_m - 1) + 2$	$S_q = \mathcal{O}_c(\frac{1}{2^q q^{2q}}N^{2q})^\dagger$
$2q$th-O-Fractal	$N = qN_1 - q + 1$	$T_{q+1} = \mathcal{O}_c(M^{rq})^\ddagger$ can reach $\mathcal{O}_c(\frac{2^q}{3^q q^{2q}}N^{2q})^\dagger$

* N is the total number of physical sensors, while N_m denotes the sensor number in the m-th subarray.
† See the proof of *Proposition 3*.
‡ Proved in (30). M and r denote the length of longest central ULA segment in the second-order difference co-array of the generator and the fractal order, respectively.

TABLE II
Examples of different structures for $q = 2$

Array Structures	$(N_1, \ldots, N_{2q})$ or N_1	Number of Sensors	Number of Consecutive Lags
4L-NA	$(3, 2, 2, 3)$	7	95
SE-4L-NA	$(3, 2, 2, 2)$	7	109
4th-O-Fractal 1	4	7	181
4th-O-Fractal 2	4	7	181
4L-NA	$(3, 3, 3, 3)$	9	215
SE-4L-NA	$(3, 3, 3, 2)$	9	235
4th-O-Fractal 3	5	9	305
4th-O-Fractal 4	5	9	379
4L-NA	$(9, 8, 8, 9)$	31	11519
SE-4L-NA	$(9, 8, 8, 8)$	31	18577
4th-O-Fractal 5	16	31	28729
4th-O-Fractal 6	16	31	21169
4th-O-Fractal 7	16	31	24805
4th-O-Fractal 8	16	31	25439

Array Structures	Type of Generator	Generator $\mathbb{G}$	r and M
4th-O-Fractal 1	MRA	$\{0, 1, 4, 6\}$	1 and 13
4th-O-Fractal 2	ENA	$\{1, 2, 5, 7\}$	1 and 13
4th-O-Fractal 3	ENA	$\{1, 2, 3, 6, 9\}$	1 and 17
4th-O-Fractal 4	INA/MRA	$\{0, 1, 4, 7, 9\}$	1 and 19
4th-O-Fractal 5	MRA	$\{0, 1, 4, 6\}$	2 and 13
4th-O-Fractal 6	ENA	$\mathbb{G}_1$ †	1 and 145
4th-O-Fractal 7	INA	$\mathbb{G}_2$ ‡	1 and 157
4th-O-Fractal 8	IMISC	$\mathbb{G}_3$ *	1 and 159

† $\mathbb{G}_1 = \{1, 2, 3, 4, 5, 6, 7, 8, 17, 25, 33, 41, 49, 57, 65, 73\}$.
‡ $\mathbb{G}_2 = \{0, 1, 2, 3, 4, 5, 6, 7, 16, 25, 34, 43, 52, 61, 70, 78\}$.
* $\mathbb{G}_3 = \{0, 2, 4, 5, 6, 10, 15, 27, 39, 51, 63, 70, 77, 79, 81, 83\}$.

B. Simulation Results for Structures with Large $2q$th-Order Difference Co-Array

Next, DOA estimation performance for structures with large $2q$th-order difference co-array is evaluated. $2q$th-O-Fractal, $2q$L-NA, and SE-$2q$L-NA with $N = 7$ physical sensors and $q = 2$ as listed in Table II are considered (here $2q$th-O-Fractal refers to 4th-O-Fractal 2 in Table II). The SS-MUSIC method [8] is employed for DOA estimation.

For the first set of simulations, the maximum number of resolvable sources of different array structures is studied.

TABLE III
EXAMPLES OF DIFFERENT STRUCTURES FOR $q = 3$

Array Structures	$(N_1, \ldots, N_{2q})$ or N_1	Number of Sensors	Number of Consecutive Lags
6L-NA	$(2, 2, 2, 2, 2, 2)$	7	191
SE-6L-NA	$(2, 2, 2, 2, 2, 1)$	7	321
6th-O-Fractal 1	3	7	427
6L-NA	$(5, 5, 5, 5, 5, 5)$	25	37499
SE-6L-NA	$(5, 5, 5, 5, 5, 4)$	25	102501
6th-O-Fractal 2	9	25	122353
6th-O-Fractal 3	9	25	137751
6th-O-Fractal 4	9	25	172315

Array Structures	Type of Generator	Generator $\mathbb{G}$	r and M
6th-O-Fractal 1	MRA	$\{0, 1, 3\}$	1 and 7
6th-O-Fractal 2	MRA	$\{0, 1, 3\}$	2 and 7
6th-O-Fractal 3	ENA	$\mathbb{G}_4$ †	1 and 51
6th-O-Fractal 4	INA	$\mathbb{G}_5$ ‡	1 and 55

† $\mathbb{G}_4 = \{1, 2, 3, 4, 5, 11, 16, 21, 26\}$.
‡ $\mathbb{G}_5 = \{0, 1, 2, 3, 8, 13, 18, 23, 27\}$.

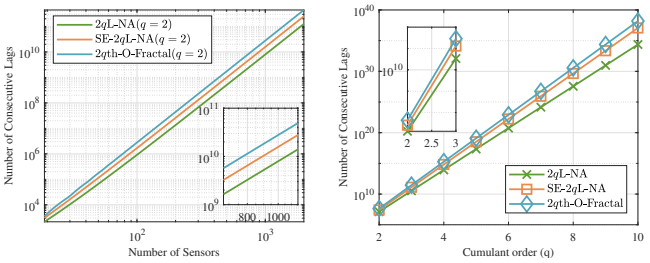

(a) Number of consecutive lags versus the number of physical sensors. (b) Number of consecutive lags versus the cumulant order q.

Fig. 3. Comparison of the number of consecutive co-array lags.

Here 45 sources are uniformly distributed between $-60°$ and $60°$. The input SNR and the number of snapshots are 20 dB and 500000, respectively. To evaluate the number of distinguishable sources, a large number of snapshots is used to calculate the fourth-order cumulant matrix [9]. The DOA estimation results for $q = 2$ are shown in Fig. 4, where it is obvious that only the $2q$th-O-Fractal is capable of resolving all the 45 sources successfully. In addition, based on the second-order difference co-array ($q = 1$), the optimized MRA with 7 physical sensors provides 35 consecutive co-array lags, which is smaller than those offered by high-order cumulants based 7-sensor arrays listed in Tables II and III. As shown in Fig. 5, MRA can only resolve up to 17 sources (equal to half of its number of consecutive co-array lags minus one). The identifiability of high-order cumulants based method is much better than that of second-order statistics based approach with a fixed sensor number.

The second set of simulations is focused on estimation accuracy. There are 10 independent sources uniformly distributed from $-60°$ to $60°$. Fig. 6(a) gives the root mean square error (RMSE) results with respect to input SNR, where the number of snapshots is fixed at 10000. As the SNR increases, the RMSE for each array structure decreases with that of the proposed $2q$th-O-Fractal ($q = 2$) being the best. The estimation performance versus the number of snapshots is

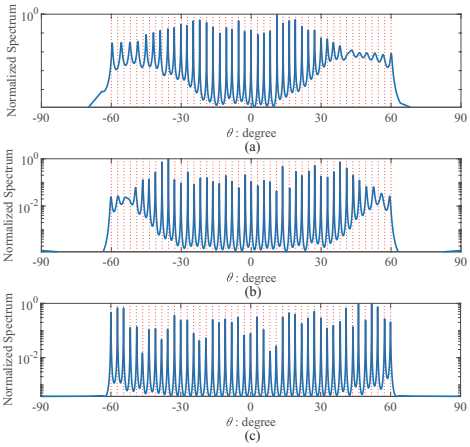

Fig. 4. DOA estimation results of different array structures. Results of (a) $2q$L-NA ($q = 2$), (b) SE-$2q$L-NA ($q = 2$), and (c) $2q$th-O-Fractal ($q = 2$).

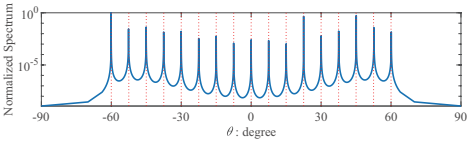

Fig. 5. DOA estimation results of MRA based on the second-order difference co-array.

shown in Fig. 6(b) with the input SNR being 20 dB. Similarly, the RMSE of each structure decreases with the increase of the snapshot number, and the best performance is achieved by the proposed $2q$th-O-Fractal ($q = 2$).

C. Comparisons of Structures Satisfying Hole-Free Property

Comparisons of array structures with the hole-free fourth-order difference co-arrays are presented next. Representative hole-free structures include 2L-FO-NA [49], CNA [50], and GCNA [51]. However, their fourth-order difference co-arrays only provide $\mathcal{O}(N^2)$ DOFs with N physical sensors. As discussed in Section IV-B, when the concatenated NA is chosen as the generator, $\mathcal{O}(N^4)$ DOFs can be achieved by the associated 4th-O-Fractal with hole-free co-array.

Fig. 7 shows the number of consecutive co-array lags versus the number of physical sensors N of 2L-FO-NA, CNA, GCNA, and 4th-O-Fractal (with concatenated NA as the generator array). The 4th-O-Fractal always achieves the largest number of consecutive co-array lags among all structures for $N \geq 15$. In addition, examples are given in Table IV for comparison, where the 4th-O-Fractal provides 1457 and 4049 consecutive lags for $N = 15$ and $N = 21$, which is superior to other structures. Note that 4th-O-Fractal in Table IV specifically refers to fractal array satisfying the sufficient condition in *Proposition 4*.

D. Simulation Results for Structures Satisfying Hole-Free Property

4th-O-Fractal (refers to 4th-O-Fractal 9), 2L-FO-NA, CNA, and GCNA with $N = 15$ physical sensors (as listed in Table IV) are involved in estimation performance comparison using the SS-MUSIC method [8]. The maximum number of

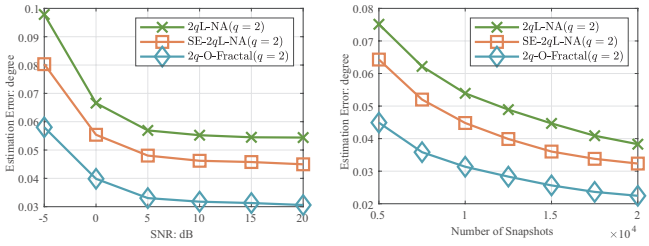

(a) RMSE versus the input SNR. (b) RMSE versus the number of snapshots.

Fig. 6. Estimation performance of different structures with holes in their difference co-arrays.

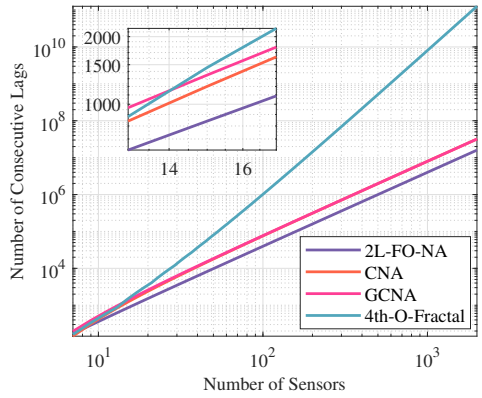

Fig. 7. Number of consecutive lags versus the number of physical sensors for different array structures satisfying the hole-free property ($q = 2$).

resolvable sources is tested. There are 52 sources uniformly distributed from $-60°$ to $60°$, and the input SNR and the number of snapshots are set as 20 dB and 50000, respectively. The DOA estimation results are shown in Fig. 8, where only the 4th-O-Fractal is capable of resolving all 52 sources successfully.

Then, consider 16 sources uniformly distributed between $-60°$ and $60°$. The RMSE versus the input SNR are shown in Fig. 9(a) with the number of snapshots fixed at 1000, while the RMSE versus the number of snapshots are given in Fig. 9(b) with the input SNR equal to 20 dB. Clearly, the proposed 4th-O-Fractal with hole-free fourth-order difference co-array outperforms other existing structures.

VI. Conclusion

Based on the $2q$th-order difference co-array, sparse array design via fractal geometries was studied, and a simple but effective systematic fractal framework was proposed. By optimizing the generator according to given requirements, a fractal array exploiting the $2q$th-order difference co-array, referred to as $2q$th-O-Fractal, was generated recursively with its properties of interest inherited from the generator, showing high flexibility in sparse array design satisfying multiple criteria. Specifically, theoretical support was given to ensure that, $\mathcal{O}(N^{2q})$ DOFs can be achieved by the proposed framework if the generator has $\mathcal{O}(N^2)$ second-order difference co-array lags. We also showed that $\mathcal{O}(N^4)$ hole-free fourth-order difference co-array lags can be achieved for $q = 2$ if the sum and difference co-arrays of the generator are hole-free. Simulation results demonstrated that by employing an optimized array as the generator, the associated fractal array generated by the proposed framework offers larger DOFs than existing structures, with better performance achieved in terms of estimation accuracy and resolution capability.

Properties of robustness and mutual coupling of the proposed framework are analyzed in the companion Part II [60]. In future work, it is interesting to further investigate

TABLE IV
Comparisons of Different Array Structures Satisfying Hole-Free Property ($q = 2$)

Array Structures	Hole-Free Co-Arrays	Number of Sensors*	Number of Consecutive Lags
2L-FO-NA	Yes	$N_1 + N_2$	$16N_1N_2 - 8N_2 + 1$
CNA	Yes	$N_1 + N_2$	M_{CN} †
GCNA	Yes	$N_1 + N_2$	M_{GCN} ‡
4th-O-Fractal	Yes	$2N_1 - 1$	$2M^{2r} - 1$

Array Structures	Number of Sensors	(N_1, N_2) or N_1	Number of Consecutive Lags
2L-FO-NA	15	$(8, 7)$	841
CNA	15	$(8, 7)$	1201
GCNA	15	$(8, 7)$	1349
4th-O-Fractal 9	15	8	1457
2L-FO-NA	21	$(11, 10)$	1681
CNA	21	$(11, 10)$	2665
GCNA	21	$(11, 10)$	2885
4th-O-Fractal 10	21	11	4049

Array Structures	Type of Generator	Generator $\mathbb{G}$	Fractal Order r and M
4th-O-Fractal 9	Concatenated NA	$\mathbb{C}_{2,4}$	1 and 27
4th-O-Fractal 10	Concatenated NA	$\mathbb{C}_{3,5}$	1 and 45

* N_m denotes the sensor number in the m-th subarray.
† $M_{\text{CN}} = 32N_1N_2 - 32N_1 - 56N_2 + 57$.
‡ $M_{\text{GCN}} = 32N_1N_2 - 8N_1 - 56N_2 + 13$.

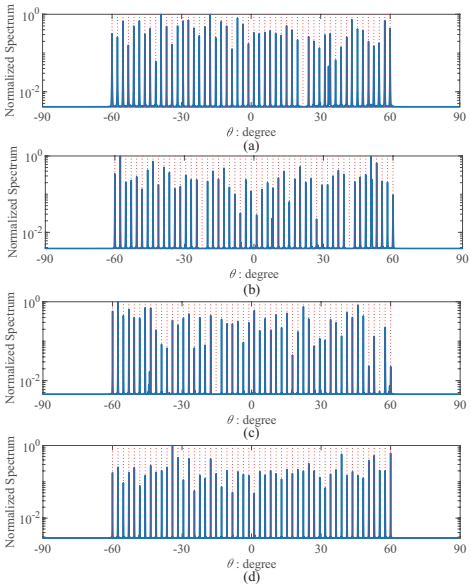

Fig. 8. DOA estimation results of different array structures satisfying hole-free property. Results of (a) 2L-FO-NA, (b) CNA, (c) GCNA, and (d) Proposed structure.

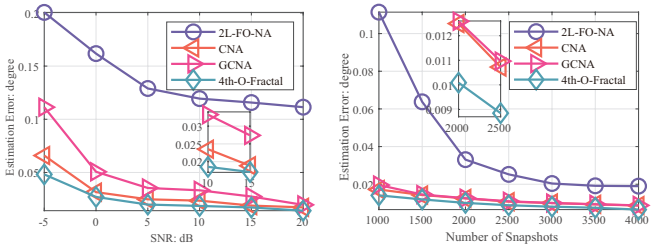

(a) RMSE versus the input SNR. (b) RMSE versus the number of snapshots.

Fig. 9. RMSE results of different array structures satisfying hole-free property.

the theoretical performance analysis of estimation methods based on high-order difference co-arrays, especially for the underdetermined case.

Appendix A
Proof of Proposition 1

We prove the proposition by mathematical induction. For $q = 1$, it can be easily obtained by the recursive expression (20) that $T_2 = M^r$. According to Theorem 1 in [3], the second-order difference co-array of SO-Fractal satisfies $\mathbb{D}_2 \supseteq \mathbb{U}_2^{'} = \left[-\frac{T_2-1}{2}, \frac{T_2-1}{2}\right]$.

For $q = p$, assume that the $2p$th-order difference co-array of $2p$th-O-Fractal satisfies

$$\mathbb{D}_{2p} \supseteq \mathbb{U}_{2p}^{'} = \left[-\frac{T_{p+1}-1}{2}, \frac{T_{p+1}-1}{2}\right]. \tag{66}$$

Then, for $q = p+1$, the $(2p+2)$th-order difference co-array of $(2p+2)$th-O-Fractal is denoted by

$$\begin{aligned}
\mathbb{D}_{2p+2} &= \left\{ \sum_{k=0}^{p} (\mu_{2k+2} - \mu_{2k+1}) \mid \mu_k \in \mathbb{E}_r^{2p+2} \right\} \\
&= \left\{ (\mu_{2p+2} - \mu_{2p+1}) - \sum_{k=0}^{p-1} (\mu_{2k+2} - \mu_{2k+1}) \mid \mu_k \in \mathbb{E}_r^{2p+2} \right\} \\
&\supseteq \left\{ (\mu_{2p+2} - \mu_{2p+1}) - s \mid \mu_k \in \mathbb{E}_r^{2p+2}, s \in \mathbb{D}_{2p} \right\}.
\end{aligned} \tag{67}$$

According to (66), denote $\phi_1 = \{(\mu_1 - \mu_2) - \mu_3 \mid \mu_1, \mu_2 \in \mathbb{E}_r^{2p+2}, \mu_3 \in \mathbb{U}_{2p}^{'}\}$ satisfying $\phi_1 \subseteq \mathbb{D}_{2p+2}$. Construct two sets $\phi_2 \subseteq \phi_1 \subseteq \mathbb{D}_{2p+2}$ and $\phi_3 \subseteq \phi_1 \subseteq \mathbb{D}_{2p+2}$, defined as

$$\begin{aligned}
\phi_2 &= \left\{ (\mu_1 - \mu_2) - \mu_3 \mid \mu_1, \mu_2 \in \mathbb{E}_{r(p+1)}, \mu_3 \in \mathbb{U}_{2p}^{'} \right\} \\
&= \left\{ (\mu_4 - \mu_5) \cdot T_{p+1} - \mu_3 \mid \mu_4, \mu_5 \in \mathbb{E}_{r(1)}, \mu_3 \in \mathbb{U}_{2p}^{'} \right\} \\
&= \left\{ \mu_6 \cdot T_{p+1} - \mu_3 \mid \mu_6 \in \mathbb{D}_2, \mu_3 \in \mathbb{U}_{2p}^{'} \right\} \\
&\supseteq \phi_2^{'} = \left\{ \mu_6 \cdot T_{p+1} - \mu_3 \mid \mu_6 \in \mathbb{U}_2^{'}, \mu_3 \in \mathbb{U}_{2p}^{'} \right\} \\
&= \left[-\frac{T_{p+1}M^r-1}{2}, \frac{T_{p+1}M^r-1}{2}\right],
\end{aligned} \tag{68}$$

$$\begin{aligned}
\phi_3 = \{&(\mu_1 - \mu_2) - \mu_3 \mid \mu_1 = f_{r(i)}T_{p+1} + m_{p+1}, \\
&\mu_2 = f_{r(j)}T_p + m_p, \mu_3 \in \mathbb{U}_{2p}^{'}\}
\end{aligned} \tag{69}$$
$$= \left\{ (f_{r(i)}T_{p+1} + m_{p+1} - f_{r(j)}T_p - m_p) - \mu_3 \mid \mu_3 \in \mathbb{U}_{2p}^{'} \right\}.$$

Substituting (21) into (69) and using *Lemma 1*, one obtains

$$\begin{aligned}
\phi_3 &= \left\{ (f_{r(i)} - f_{r(j)})(T_{p+1} + T_p) - \mu_3 \mid \mu_3 \in \mathbb{U}_{2p}^{'} \right\} \\
&= \left\{ (M^r - 1)\tfrac{T_{p+1}+T_p}{2} - \mu_3 \mid \mu_3 \in \mathbb{U}_{2p}^{'} \right\} \\
&= \left[\tfrac{T_{p+1}(M^r-2)+T_p(M^r-1)+1}{2}, \tfrac{T_{p+1}M^r+T_p(M^r-1)-1}{2} \right].
\end{aligned} \tag{70}$$

The upper bound of the set $\phi_2^{'}$ is always greater than the lower bound of ϕ_3 since

$$\begin{aligned}
&(T_{p+1}M^r - 1) - \left[T_{p+1}(M^r - 2) + T_p(M^r - 1) + 1\right] \\
&= 2T_{p+1} - T_pM^r + T_p - 2, \\
&= T_pM^r + 2T_{p-1}(M^r - 1) + T_p - 2 > 0,
\end{aligned} \tag{71}$$

where (20) is substituted to obtain the final result at the last step. Therefore, the union of $\phi_2^{'}$ and ϕ_3 is

$$\phi_2^{'} \cup \phi_3 = \left[-\tfrac{T_{p+1}M^r-1}{2}, \tfrac{T_{p+1}M^r+T_p(M^r-1)-1}{2} \right]. \tag{72}$$

Due to the symmetric property of difference co-arrays, and the relationships $\phi_2^{'} \subseteq \phi_2 \subseteq \mathbb{D}_{2p+2}$ and $\phi_3 \subseteq \mathbb{D}_{2p+2}$, one has

$$\mathbb{D}_{2p+2} \supseteq \left[-\tfrac{T_{p+1}M^r+T_p(M^r-1)-1}{2}, \tfrac{T_{p+1}M^r+T_p(M^r-1)-1}{2} \right]. \tag{73}$$

From (20),

$$T_{p+2} = T_{p+1}M^r + T_p(M^r - 1). \tag{74}$$

Finally, (73) is simplified to

$$\mathbb{D}_{2p+2} \supseteq \left[-\tfrac{T_{p+2}-1}{2}, \tfrac{T_{p+2}-1}{2}\right] = \mathbb{U}_{2p+2}^{'}, \tag{75}$$

which completes the proof.

References

[1] H. L. V. Trees, *Optimum Array Processing: Part IV of Detection, Estimation, and Modulation Theory*. John Wiley & Sons, Apr. 2004.

[2] P. Pal and P. P. Vaidyanathan, "Nested arrays: A novel approach to array processing with enhanced degrees of freedom," *IEEE Trans. Signal Process.*, vol. 58, no. 8, pp. 4167–4181, 2010.

[3] R. Cohen and Y. C. Eldar, "Sparse array design via fractal geometries," *IEEE Trans. Signal Process.*, vol. 68, pp. 4797–4812, 2020.

[4] H. Dai, Z. Zhang, S. Gong, C. Xing, and J. An, "Training optimization for subarray based IRS-assisted MIMO communications," *IEEE Internet Things J.*, vol. 9, no. 4, pp. 2890–2905, Feb. 2022.

[5] P. P. Vaidyanathan and P. Pal, "Sparse sensing with co-prime samplers and arrays," *IEEE Trans. Signal Process.*, vol. 59, no. 2, pp. 573–586, Feb. 2011.

[6] Q. Shen, W. Liu, W. Cui, and S. Wu, "Underdetermined DOA estimation under the compressive sensing framework: A review," *IEEE Access*, vol. 4, pp. 8865–8878, 2016.

[7] C.-L. Liu and P. P. Vaidyanathan, "Maximally economic sparse arrays and Cantor arrays," in *Proc. IEEE Int. Workshop Comput. Advances MultiSensor Adaptive Process.*, Dec. 2017, pp. 1–5.

[8] P. Pal and P. P. Vaidyanathan, "Multiple level nested array: An efficient geometry for 2qth order cumulant based array processing," *IEEE Trans. Signal Process.*, vol. 60, no. 3, pp. 1253–1269, Mar. 2012.

[9] Q. Shen, W. Liu, W. Cui, S. Wu, and P. Pal, "Simplified and enhanced multiple level nested arrays exploiting high-order difference co-arrays," *IEEE Trans. Signal Process.*, vol. 67, no. 13, pp. 3502–3515, Jul. 2019.

[10] A. Moffet, "Minimum-redundancy linear arrays," *IEEE Trans. Antennas Propagat.*, vol. 16, no. 2, pp. 172–175, Mar. 1968.

[11] P. Pal and P. P. Vaidyanathan, "Coprime sampling and the MUSIC algorithm," in *Proc. IEEE Digit. Signal Process. Signal Process. Educ. Meeting*, Jan. 2011, pp. 289–294.

[12] M. Yang, L. Sun, X. Yuan, and B. Chen, "Improved nested array with hole-free DCA and more degrees of freedom," *Electron. lett.*, vol. 52, no. 25, pp. 2068–2070, Dec. 2016.

[13] P. Zhao, G. Hu, Z. Qu, and L. Wang, "Enhanced nested array configuration with hole-free co-array and increasing degrees of freedom for DOA estimation," *IEEE Commun. Lett.*, vol. 23, no. 12, pp. 2224–2228, Dec. 2019.

[14] Z. Zheng, W.-Q. Wang, Y. Kong, and Y. D. Zhang, "MISC array: A new sparse array design achieving increased degrees of freedom and reduced mutual coupling effect," *IEEE Trans. Signal Process.*, vol. 67, no. 7, pp. 1728–1741, Apr. 2019.

[15] W. Shi, Y. Li, and R. C. de Lamare, "Novel Sparse Array Design Based on the Maximum Inter-Element Spacing Criterion," *IEEE Signal Process. Lett.*, pp. 1–5, 2022.

[16] C.-L. Liu and P. P. Vaidyanathan, "Remarks on the spatial smoothing step in coarray MUSIC," *IEEE Signal Process. Lett.*, vol. 22, no. 9, pp. 1438–1442, Sep. 2015.

[17] X. Wang and X. Wang, "Hole identification and filling in k-times extended co-prime arrays for highly efficient DOA estimation," *IEEE Trans. Signal Process.*, vol. 67, no. 10, pp. 2693–2706, May 2019.

[18] W. Zheng, X. Zhang, Y. Wang, J. Shen, and B. Champagne, "Padded coprime arrays for improved DOA estimation: Exploiting hole representation and filling strategies," *IEEE Trans. Signal Process.*, vol. 68, pp. 4597–4611, 2020.

[19] P. Ma, J. Li, F. Xu, and X. Zhang, "Hole-free coprime array for DOA estimation: Augmented uniform co-array," *IEEE Signal Process. Lett.*, vol. 28, pp. 36–40, 2021.

[20] W. Zheng, X. Zhang, J. Li, and J. Shi, "Extensions of co-prime array for improved DOA estimation with hole filling strategy," *IEEE Sensors J.*, vol. 21, no. 5, pp. 6724–6732, Mar. 2021.

[21] S. Qin and Y. D. Zhang, "Generalized coprime array configurations for direction-of-arrival estimation," *IEEE Trans. Signal Process.*, vol. 63, no. 6, pp. 1377–1390, Mar. 2015.

[22] T. Svantesson, "Modeling and estimation of mutual coupling in a uniform linear array of dipoles," in *Proc. IEEE Int. Conf. Acoust., Speech, Signal Process.*, 1999, pp. 2961–2964.

[23] C.-L. Liu and P. P. Vaidyanathan, "Super nested arrays: Linear sparse arrays with reduced mutual coupling—Part I: Fundamentals," *IEEE Trans. Signal Process.*, vol. 64, no. 15, pp. 3997–4012, Aug. 2016.

[24] ——, "Super nested arrays: Linear sparse arrays with reduced mutual coupling—Part II: High-order extensions," *IEEE Trans. Signal Process.*, vol. 64, no. 16, pp. 4203–4217, Aug. 2016.

[25] J. Liu, Y. Zhang, Y. Lu, S. Ren, and S. Cao, "Augmented nested arrays with enhanced DOF and reduced mutual coupling," *IEEE Trans. Signal Process.*, vol. 65, no. 21, pp. 5549–5563, Nov. 2017.

[26] A. Raza, W. Liu, and Q. Shen, "Thinned coprime array for second-order difference co-array generation with reduced mutual coupling," *IEEE Trans. Signal Process.*, vol. 67, no. 8, pp. 2052–2065, Apr. 2019.

[27] C.-L. Liu and P. P. Vaidyanathan, "Robustness of difference coarrays of sparse arrays to sensor failures—Part I: A theory motivated by coarray MUSIC," *IEEE Trans. Signal Process.*, vol. 67, no. 12, pp. 3213–3226, Jun. 2019.

[28] ——, "Robustness of difference coarrays of sparse arrays to sensor failures—Part II: Array geometries," *IEEE Trans. Signal Process.*, vol. 67, no. 12, pp. 3227–3242, Jun. 2019.

[29] C.-L. Liu and P. Vaidyanathan, "Novel algorithms for analyzing the robustness of difference coarrays to sensor failures," *Signal Process.*, vol. 171, p. 107517, Jun. 2020.

[30] C.-L. Liu and P. P. Vaidyanathan, "Optimizing minimum redundancy arrays for robustness," in *Proc. IEEE Asilomar Conf. Signals, Syst., Comput.*, Oct. 2018, pp. 79–83.

[31] ——, "Composite Singer arrays with hole-free coarrays and enhanced robustness," in *Proc. IEEE Int. Conf. Acoust., Speech, Signal Process.*, May 2019, pp. 4120–4124.

[32] D. Zhu, S. Wang, and G. Li, "Multiple-fold redundancy arrays with robust difference coarrays: Fundamental and analytical design method," *IEEE Trans. Antennas Propagat.*, vol. 69, no. 9, pp. 5570–5584, Sep. 2021.

[33] K. J. Falconer, *Fractal Geometry: Mathematical Foundations and Applications*. John Wiley & Sons Inc, 2014.

[34] D. Werner, R. Haupt, and P. Werner, "Fractal antenna engineering: The theory and design of fractal antenna arrays," *IEEE Antennas Propag. Mag.*, vol. 41, no. 5, pp. 37–58, Oct. 1999.

[35] D. Werner and S. Ganguly, "An overview of fractal antenna engineering research," *IEEE Antennas Propag. Mag.*, vol. 45, no. 1, pp. 38–57, Feb. 2003.

[36] C. Puente-Baliarda and R. Pous, "Fractal design of multiband and low side-lobe arrays," *IEEE Trans. Antennas Propagat.*, vol. 44, no. 5, p. 730, May 1996.

[37] R. Cohen and Y. C. Eldar, "Sparse fractal array design with increased degrees of freedom," in *Proc. IEEE Int. Conf. Acoust., Speech, Signal Process.*, May 2019, pp. 4195–4199.

[38] B. Porat and B. Friedlander, "Direction finding algorithms based on high-order statistics," *IEEE Trans. Signal Process.*, vol. 39, no. 9, pp. 2016–2024, Sep. 1991.

[39] C. Nikias and J. Mendel, "Signal processing with higher-order spectra," *IEEE Signal Process. Mag.*, vol. 10, no. 3, pp. 10–37, Jul. 1993.

[40] M. Dogan and J. Mendel, "Applications of cumulants to array processing—Part I: Aperture extension and array calibration," *IEEE Trans. Signal Process.*, vol. 43, no. 5, pp. 1200–1216, May 1995.

[41] E. Gonen and J. Mendel, "Applications of cumulants to array processing—Part VI: Polarization and direction of arrival estimation with minimally constrained arrays," *IEEE Trans. Signal Process.*, vol. 47, no. 9, pp. 2589–2592, Sep. 1999.

[42] P. Chevalier and A. Ferreol, "On the virtual array concept for the fourth-order direction finding problem," *IEEE Trans. Signal Process.*, vol. 47, no. 9, pp. 2592–2595, Sep. 1999.

[43] P. Chevalier, L. Albera, A. Ferreol, and P. Comon, "On the virtual array concept for higher order array processing," *IEEE Trans. Signal Process.*, vol. 53, no. 4, pp. 1254–1271, Apr. 2005.

[44] P. Chevalier, A. Ferreol, and L. Albera, "High-resolution direction finding from higher order statistics: The $2q$-MUSIC algorithm," *IEEE Trans. Signal Process.*, vol. 54, no. 8, pp. 2986–2997, Aug. 2006.

[45] Jin Ho Choi and C. D. Yoo, "Underdetermined High-Resolution DOA Estimation: A 2ρ th-Order Source-Signal/Noise Subspace Constrained Optimization," *IEEE Trans. Signal Process.*, vol. 63, no. 7, pp. 1858–1873, Apr. 2015.

[46] J. He, Z. Zhang, C. Gu, T. Shu, and W. Yu, "Cumulant-Based 2-D Direction Estimation Using an Acoustic Vector Sensor Array," *IEEE Trans. Aerosp. Electron. Syst.*, vol. 56, no. 2, pp. 956–971, Apr. 2020.

[47] J. Cai, W. Liu, R. Zong, and Q. Shen, "An expanding and shift scheme for constructing fourth-order difference coarrays," *IEEE Signal Process. Lett.*, vol. 24, no. 4, pp. 480–484, Apr. 2017.

[48] Q. Shen, W. Liu, W. Cui, and S. Wu, "Extension of nested arrays with the fourth-order difference co-array enhancement," in *Proc. IEEE Int. Conf. Acoust., Speech, Signal Process.*, Mar. 2016, pp. 2991–2995.

[49] A. Ahmed, Y. D. Zhang, and B. Himed, "Effective nested array design for fourth-order cumulant-based DOA estimation," in *Proc. IEEE Radar Conf.*, May 2017, pp. 998–1002.

[50] Y. Zhou, Y. Li, L. Wang, C. Wen, and W. Nie, "The compressed nested array for underdetermined DOA estimation by fourth-order difference coarrays," in *Proc. IEEE Int. Conf. Acoust., Speech, Signal Process.*, May 2020, pp. 4617–4621.

[51] B. Dang and Y. Zhou, "The generalized compressed nested array for the construction of fourth-order difference co-array," *Circuits Syst Signal Process*, vol. 40, no. 12, pp. 6340–6353, Dec. 2021.

[52] Z. Yang, Q. Shen, W. Liu, Y. C. Eldar, and W. Cui, "Extended Cantor arrays with hole-free fourth-order difference co-arrays," in *Proc. IEEE Int. Symp. Circuits Syst.*, May 2021, pp. 1–5.

[53] J. M. Mendel, "Tutorial on higher-order statistics (spectra) in signal processing and system theory: Theoretical results and some applications," *Proc. IEEE*, vol. 79, no. 3, pp. 278–305, Mar. 1991.

[54] Q. Shen, W. Liu, W. Cui, and S. Wu, "Extension of co-prime arrays based on the fourth-order difference co-array concept," *IEEE Signal Process. Lett.*, vol. 23, no. 5, pp. 615–619, May 2016.

[55] Q. Shen, W. Liu, W. Cui, S. Wu, Y. D. Zhang, and M. G. Amin, "Low-complexity direction-of-arrival estimation based on wideband co-prime arrays," *IEEE/ACM Trans. Audio, Speech, Language Process.*, vol. 23, no. 9, pp. 1445–1456, Sep. 2015.

[56] ——, "Focused compressive sensing for underdetermined wideband DOA estimation exploiting high-order difference coarrays," *IEEE Signal Process. Lett.*, vol. 24, no. 1, pp. 86–90, Jan. 2017.

[57] W. Cui, Q. Shen, W. Liu, and S. Wu, "Low complexity DOA estimation for wideband off-grid sources based on re-focused compressive sensing with dynamic dictionary," *IEEE J. Sel. Top. Signal Process.*, vol. 13, no. 5, pp. 918–930, Sep. 2019.

[58] C.-L. Liu, P. P. Vaidyanathan, and P. Pal, "Coprime coarray interpolation for DOA estimation via nuclear norm minimization," in *Proc. IEEE Int. Symp. Circuits Syst.*, May 2016, pp. 2639–2642.

[59] C. Zhou, Y. Gu, X. Fan, Z. Shi, G. Mao, and Y. D. Zhang, "Direction-of-arrival estimation for coprime array via virtual array interpolation," *IEEE Trans. Signal Process.*, vol. 66, no. 22, pp. 5956–5971, Nov. 2018.

[60] Z. Yang, Q. Shen, W. Liu, Y. C. Eldar, and W. Cui, "High-order cumulants based sparse array design via fractal geometries—Part II: Robustness and mutual coupling," *IEEE Trans. Signal Process.*, submitted.

[61] Y.-P. Chen and C.-L. Liu, "On the size and redundancy of the fourth-order difference co-array," *IEEE Signal Process. Lett.*, vol. 28, pp. 2013–2017, 2021.
[62] M. F. Challis, H. House, L. G. Hempnall, and J. P. Robinson, "Some extremal postage stamp bases," *J. Integer Seq.*, vol. 13, no. 2, p. 3, 2010.
[63] J. Kohonen, "A meet-in-the-middle algorithm for finding extremal restricted additive 2-bases," *J. Integer Seq.*, vol. 17, no. 6, pp. 14–6, 2014.
[64] R. Rajamäki and V. Koivunen, "Sparse symmetric linear arrays with low redundancy and a contiguous sum co-array," *IEEE Trans. Signal Process.*, vol. 69, pp. 1697–1712, 2021.
[65] Z. Fu, P. Charge, and Y. Wang, "A virtual nested MIMO array exploiting fourth order difference coarray," *IEEE Signal Process. Lett.*, vol. 27, pp. 1140–1144, 2020.
[66] J. Kohonen, "Early pruning in the restricted postage stamp problem," *arXiv preprint arXiv:1503.03416*, 2015.

Zixiang Yang received the B.S. degree in electronic and information engineering from the University of Electronic Science and Technology of China, Chengdu, China, in 2017. He is currently working toward the Ph.D. degree with the School of Information and Electronics, Beijing Institute of Technology, Beijing, China. His research interests include array signal processing and radar signal processing.

Qing Shen received his B.S. degree in 2009 and Ph.D. degree in 2016, both from the Beijing Institute of Technology, Beijing, China. He then worked as a Postdoctoral Researcher with the Beijing Institute of Technology, where he is currently an Associate Professor. From 2013 to 2015 and from 2018 to 2019, he was a Sponsored Researcher in the Department of Electronic and Electrical Engineering, University of Sheffield, Sheffield, UK. His research interests include sensor array signal processing, statistical signal processing, adaptive signal processing, and their various applications to acoustics, radar, sonar, and wireless communications. He was the recipient of two Excellent Ph.D. Thesis Awards from both the Chinese Institute of Electronics and the Beijing Institute of Technology in 2016. He was also the recipient of the Second-Class Prize of the National Award for Technological Invention in 2020, the First-Class Prize of the Science and Technology (Technological Invention) Award from the Chinese Institute of Electronics in 2018, the Second-Class Prize of the Ministerial Level Science and Technology Progress Award in 2014, and the Young Scientist Award from the IEEE ICET 2021. He is currently a member of the Digital Signal Processing Technical Committee of the IEEE Circuits and Systems Society. He is the Financial Co-Chair of the IEEE CAMSAP 2023, and served as the Session Co-Chair of several international conferences.

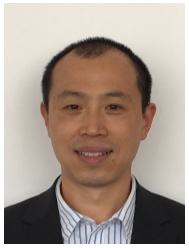

Wei Liu (S'01-M'04-SM'10) received his BSc and LLB. degrees from Peking University, China, in 1996 and 1997, respectively, MPhil from the University of Hong Kong in 2001, and PhD from University of Southampton, UK, in 2003. He then worked as a postdoc first at Southampton and later at Imperial College London. Since September 2005, he has been with the Department of Electronic and Electrical Engineering, University of Sheffield, UK, first as a Lecturer and then a Senior Lecturer. He has published 380+ journal and conference papers, five book chapters, and two research monographs titled "Wideband Beamforming: Concepts and Techniques" (Wiley, March 2010) and "Low-Cost Smart Antennas" (Wiley, March 2019), respectively. His research interests cover a wide range of topics in signal processing, with a focus on sensor array signal processing and its various applications, such as robotics and autonomous systems, human computer interface, radar, sonar, and wireless communications. He is a member of the Digital Signal Processing Technical Committee of the IEEE Circuits and Systems Society (Chair from May 2022) and the Sensor Array and Multichannel Signal Processing Technical Committee of the IEEE Signal Processing Society (Chair for 2021-2022). He was an Associate Editor for IEEE Trans. on Signal Processing (2015-2019) and IEEE Access (2016-2021), and is currently an editorial board member of the journals Frontiers of Information Technology and Electronic Engineering and Journal of the Franklin Institute.

Yonina C. Eldar (S'98-M'02-SM'07-F'12) received the B.Sc. degree in Physics in 1995 and the B.Sc. degree in Electrical Engineering in 1996 both from Tel-Aviv University (TAU), Tel-Aviv, Israel, and the Ph.D. degree in Electrical Engineering and Computer Science in 2002 from the Massachusetts Institute of Technology (MIT), Cambridge. She is currently a Professor in the Department of Mathematics and Computer Science, Weizmann Institute of Science, Rehovot, Israel. She was previously a Professor in the Department of Electrical Engineering at the Technion. She is also a Visiting Professor at MIT, a Visiting Scientist at the Broad Institute, and an Adjunct Professor at Duke University and was a Visiting Professor at Stanford. She is a member of the Israel Academy of Sciences and Humanities (elected 2017), an IEEE Fellow and a EURASIP Fellow. Her research interests are in the broad areas of statistical signal processing, sampling theory and compressed sensing, learning and optimization methods, and their applications to biology, medical imaging and optics.

Dr. Eldar has received many awards for excellence in research and teaching, including the IEEE Signal Processing Society Technical Achievement Award (2013), the IEEE/AESS Fred Nathanson Memorial Radar Award (2014), and the IEEE Kiyo Tomiyasu Award (2016). She was a Horev Fellow of the Leaders in Science and Technology program at the Technion and an Alon Fellow. She received the Michael Bruno Memorial Award from the Rothschild Foundation, the Weizmann Prize for Exact Sciences, the Wolf Foundation Krill Prize for Excellence in Scientific Research, the Henry Taub Prize for Excellence in Research (twice), the Hershel Rich Innovation Award (three times), the Award for Women with Distinguished Contributions, the Andre and Bella Meyer Lectureship, the Career Development Chair at the Technion, the Muriel & David Jacknow Award for Excellence in Teaching, and the Technion's Award for Excellence in Teaching (two times). She received several best paper awards and best demo awards together with her research students and colleagues including the SIAM outstanding Paper Prize, the UFFC Outstanding Paper Award, the Signal Processing Society Best Paper Award and the IET Circuits, Devices and Systems Premium Award, was selected as one of the 50 most influential women in Israel and in Asia, and is a highly cited researcher.

She was a member of the Young Israel Academy of Science and Humanities and the Israel Committee for Higher Education. She is the Editor in Chief of Foundations and Trends in Signal Processing, a member of the IEEE Sensor Array and Multichannel Technical Committee and serves on several other IEEE committees. In the past, she was a Signal Processing Society Distinguished Lecturer, member of the IEEE Signal Processing Theory and Methods and Bio Imaging Signal Processing technical committees, and served as an associate editor for the IEEE Transactions On Signal Processing, the EURASIP Journal of Signal Processing, the SIAM Journal on Matrix Analysis and Applications, and the SIAM Journal on Imaging Sciences. She was Co-Chair and Technical Co-Chair of several international conferences and workshops. She is author of the book "Sampling Theory: Beyond Bandlimited Systems" and co-author of five other books published by Cambridge University Press.

Wei Cui received the B.S. degree in physics and Ph.D. degree in Electronics Engineering from Beijing Institute of Technology, Beijing, China, in 1998 and 2003, respectively. From March 2003 to March 2005, he worked as a Post-Doctor in the School of Electronic and Information Engineering, Beijing Jiaotong University. Since then, he has been with the Beijing Institute of Technology, where he is currently a Professor with the School of Information and Electronics. His research interests include adaptive signal processing, array signal processing, sparse signal processing, and their various applications such as Radar, aerospace telemetry tracking and command. He has published more than 100 papers, holds 52 patents, and received the Ministerial Level Technology Advancement Award twice.